Chapter 4 Supersymmetry Studies at the Linear Collider

1 Introduction

The Standard Model (SM) has been tested by a spectacularly large and diverse set of experiments. The resulting body of data is consistent with the matter content and gauge interactions of the SM with a Higgs boson of mass $m_h \lesssim 250$ GeV [1]. If a fundamental Higgs boson exists, it fits much more naturally into supersymmetric extensions of the SM than into the SM itself [2–5]. Thus, the study of supersymmetry (SUSY) is among the highest priorities for future accelerators.

If SUSY exists, many of its most important motivations suggest that at least some superpartners have masses below about 1 TeV. These motivations, ranging from gauge coupling unification [6–10] to the existence of an excellent dark matter candidate [11], are discussed in previous chapters and also below. While none of these is a guarantee of SUSY, they all provide motivation for the presence of SUSY at the weak-interaction scale.

In the supersymmetric extension of the SM with minimal field content, hundreds of additional parameters enter the Lagrangian. If SUSY is discovered, this discovery will open new questions—to understand the pattern of the SUSY parameters, to determine from them the mechanism of SUSY breaking, and to infer from them the nature of physics at the very highest energy scales. Such grand goals may be contemplated only if precise and model-independent measurements of superpartner properties are possible.

In this chapter, we describe the prospects for such measurements at a 0.5–1.0 TeV e^+e^- linear collider (LC) with longitudinally polarized electron beams. The potential of linear colliders for detailed studies of supersymmetry has been discussed previously in numerous reports [12–18]. In this chapter, many well-established results are reviewed, including the potential for model-independent measurements of superpartner masses. In addition, several less well-appreciated topics are discussed. These include loop-level effects in supersymmetry, CP violation, and supersymmetric flavor violation. This discussion serves both to illustrate the rich program of supersymmetric studies available at linear colliders, and to highlight areas that merit further study. This chapter concludes with a review of the important complementarity of the LC and the Large Hadron Collider (LHC) with respect to supersymmetry studies.

The signatures of supersymmetry are many, ranging from the well-known missing energy in supergravity with R-parity conservation [19,20] to exotic signatures appearing in models with gauge-mediated [21] and anomaly-mediated [22,23] supersymmetry breaking. Space constraints prevent a complete review of the considerable work done

in each of these, and other, frameworks. Instead, this review focuses on supergravity frameworks leading to the conventional signature of missing energy. R-parity violation and alternative supersymmetry-breaking mechanisms are treated as variations, and are discussed where they are especially pertinent.

2 The scale of supersymmetry

The cleanliness of the linear collider environment implies that precise, model-independent measurements in supersymmetry are possible, but only if supersymmetric final states are kinematically accessible. The mass scale of supersymmetric particles is therefore of paramount importance. In this section we review bounds on superpartner masses from naturalness criteria, dark matter constraints, Higgs boson searches, and precision electroweak data. We also consider the potential of experimental evidence for new physics to constrain the supersymmetric mass scale; we discuss the muon anomalous magnetic moment as an example.

2.1 Naturalness

In supersymmetric extensions of the SM, quadratically divergent quantum corrections to the masses of fundamental scalars are of the order of the superpartner mass scale. Given a mechanism for producing sufficiently light superpartners, the observed weak scale is obtained without unnaturally large cancellations in the electroweak potential. While no analysis of naturalness can claim quantitative rigor, the importance of naturalness as a fundamental motivation for supersymmetry has prompted many studies [24–46], with important qualitative implications for the superparticle spectrum.

To study naturalness one must first assume a certain supersymmetric framework. Models in this framework are specified by a set of input parameters, typically defined at some high energy scale. Together with experimental constraints and renormalization group equations, these parameters determine the entire weak-scale Langrangian, including the Z boson mass, which at tree level is

$$\frac{1}{2}m_Z^2 = \frac{m_{H_d}^2 - m_{H_u}^2 \tan^2\beta}{\tan^2\beta - 1} - \mu^2 \ , \tag{4.1}$$

where $m_{H_d}^2$, $m_{H_u}^2$ are the mass parameters of the two Higgs doublets of the model and $\tan\beta = \langle H_u \rangle / \langle H_d \rangle$. Naturalness is then often imposed by demanding that the weak scale be insensitive to variations in some set of parameters a_i, which are assumed to be continuously variable, independent, and fundamental. The a_i may be scalar masses, gaugino masses, and other parameters, but are not necessarily input parameters. The sensitivity is typically quantified by defining coefficients [24,25]

$c_i \equiv |(a_i/m_Z)(\partial m_Z/\partial a_i)|$ for each parameter a_i and taking some simple combination of the c_i, often $c = \max\{c_i\}$, as an overall measure of naturalness. A naturalness criterion $c < c_{\rm max}$ then implies upper bounds on supersymmetry parameters and superpartner masses.

Following the early studies [24,25], the authors of [27] stressed the importance of including one-loop corrections to Eq. (4.1). They also noted that it is possible in principle for a given c_i to be large for all possible choices of a_i. In the latter case, the authors of [28–30] argued that, to avoid misleading results, only *unusually* large sensitivity should be considered unnatural and proposed replacing c by $\tilde{\gamma} \equiv \max\{c_i/\overline{c}_i\}$, with $\overline{c}_i$ an average sensitivity. More recently, another alternative prescription has been proposed [34–38] in which the sensitivity coefficients are replaced by $|(\Delta a_i/m_Z)(\partial m_Z/\partial a_i)|$, where Δa_i is the experimentally allowed range of a_i. This definition implies that arbitrarily large but well-measured supersymmetry parameters are natural, and has been argued to differ sharply from conventional notions of naturalness [46].

The results of naturalness studies are strongly dependent on the choice of framework, the choice of fundamental parameters a_i, and, of course, the choice of $c_{\rm max}$ (or the equivalent $\tilde{\gamma}$ parameter). The dependence on framework assumptions is inescapable. In other studies of supersymmetry there exists, at least in principle, the possibility of a model-independent study, where no correlations among parameters are assumed. In studies of naturalness, however, the correlations determine the results, and there is no possibility, even in principle, of an all-inclusive framework. We describe here only some of the qualitatively distinct possibilities. For alternative analyses, readers are referred to the original literature [24–46].

In minimal supergravity, one assumes both scalar and gaugino universality at a high scale. If one requires insensitivity of the weak scale with respect to both supersymmetry breaking and Standard Model parameters, none of the superpartner masses can naturally be far above the weak scale. Examples of the resulting naturalness bounds are given in Fig. 4.1. The bounds for non-strongly interacting superpartners are typically more stringent than those for colored superpartners. Similar results are found in other frameworks where all scalar and gaugino masses are comparable at some high scale.

Naturalness bounds may be very different in other frameworks, however, especially for scalars. For squark and slepton masses, if no correlations are assumed, the bounds are highly generation-dependent. At one-loop, the weak scale is sensitive to sfermion masses only through renormalization group terms proportional to Yukawa couplings. Thus, while the scalar masses of the third generation are still usefully constrained by naturalness criteria, first- and second-generation scalars may have masses above 10 TeV without requiring large fine-tuning [31,32], putting them far beyond the kinematic reaches of both the LHC and future linear colliders. 'Superheavy' first and second generation scalars ameliorate the supersymmetric flavor and CP problems and

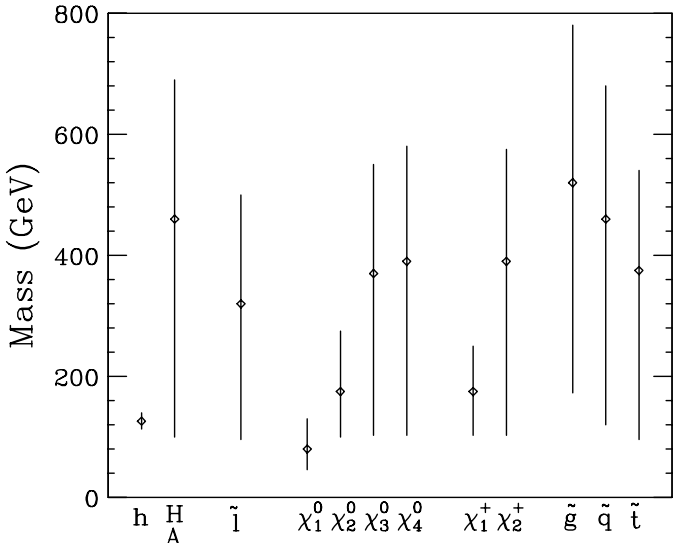

Figure 4.1: Natural ranges of superpartner masses in minimal supergravity. The upper limits are set by the requirement $\tilde{\gamma} < 10$ and the diamonds indicate upper bounds corresponding to $\tilde{\gamma} < 5$. The lower limits are roughly those from current collider constraints. Updated from [29].

are found in many models [47–63].

Alternatively, given the possibility that SM couplings are fixed in sectors separate from supersymmetry breaking, one may reasonably require only that the weak scale be insensitive to variations in parameters related to supersymmetry breaking [44–46]. With this less stringent criterion, in many simple models, including minimal supergravity, all scalar partners may be naturally in the 2–3 TeV range, as a result of focusing behavior in renormalization group trajectories [44–46,64–68]. Such "focus point supersymmetry" models also have significant virtues with respect to low-energy constraints, and predict that even third-generation scalars may have masses well above 1 TeV and be beyond the reach of linear colliders.

Bounds on the masses of fermionic superpartners are less framework-dependent. If the gaugino masses are uncorrelated, the gluino mass is typically stringently bounded by its indirect influence on the weak scale through the top squarks. In this general context, the electroweak gaugino masses may be significantly larger [42,43]. However, in most well-motivated models, the gluino is much heavier than the electroweak gauginos, and so naturalness implies stringent limits on Bino and Wino masses. While the scale of the μ parameter may be determined [69], a quantitative theory for the μ term is lacking. The μ parameter is therefore usually determined through Eq. (4.1) and is otherwise assumed to be uncorrelated with other parameters. Large μ then necessarily leads to large fine-tuning, and so heavy Higgsinos are disfavored. As a result, given our present understanding, naturalness criteria typically imply relatively stringent bounds on the masses of all six chargino and neutralino states, and they

encourage the expectation that all of these particles will be available for study at linear colliders.

2.2 Neutralino relic abundance

An important virtue of many supersymmetric theories is the existence of a non-baryonic dark matter candidate. The most straightforward possibility is the lightest neutralino χ [11,70], which is often the lightest supersymmetric particle (LSP) and so is stable in models with conserved R-parity. Current cosmological and astrophysical measurements prefer $0.1 \lesssim \Omega_m h^2 \lesssim 0.3$ [71], where Ω_m is the ratio of dark matter density to critical density, and $h \approx 0.65$ is the Hubble parameter in units of $100\,\mathrm{km\,s^{-1}\,Mpc^{-1}}$. The superpartner spectrum is then constrained by the requirement that the thermal relic density of the lightest neutralino satisfy $\Omega_\chi h^2 \lesssim 0.3$.

The neutralino relic density is determined by the neutralino pair annihilation cross section and has been the subject of many analyses [72–100]. These include refined treatments of poles [72–74], annihilation thresholds [72,73], and co-annihilation among Higgsinos [75] and with staus [76,77]. The S- and P-wave contributions to all tree-level processes with two-body final states are given in [78].

In general, neutralinos may annihilate through t-channel sfermions to $f\overline{f}$, through s-channel Z and Higgs bosons to $f\overline{f}$, and through t-channel charginos and neutralinos to WW and ZZ. For Bino dark matter, only the sfermion-mediated amplitudes are non-vanishing. An upper bound on $\Omega_\chi h^2$ then leads to an upper bound on at least one sfermion mass. This, together with the requirement that χ be the LSP, implies an upper bound on m_χ. Such reasoning has led to claims of cosmological upper bounds on superpartner masses with optimistic implications for supersymmetry at linear colliders [79–89].

These claims must be viewed cautiously, however, as they are true only in the $\chi \approx \tilde{B}$ limit and are violated even in the simplest scenarios. In minimal supergravity, for example, multi-TeV LSPs are possible for large m_0 [94], where the LSP has a significant Higgsino admixture, leading to large annihilation cross sections to gauge bosons. Useful upper bounds are also absent in minimal supergravity at large $\tan\beta$ [94–97], where the importance of a small Higgsino admixture in χ is amplified and leads to large Higgs boson-mediated annihilation. More generally, no guarantee of light superpartners is possible for Wino- [98–100] and Higgsino-like [75,90] LSPs, which annihilate very efficiently to negligible relic densities. Finally, it is worth recalling that these upper bounds are also inapplicable in theories with low-energy supersymmetry breaking or R-parity violation, where the lightest neutralino is no longer stable.

2.3 Higgs mass and precision electroweak constraints

As is well known, supersymmetry places severe constraints on the mass of the lightest Higgs boson. In the Minimal Supersymmetric Standard Model (MSSM), one-loop calculations [101–110] have now been supplemented with leading two-loop corrections in the Feynman diagrammatic [111–115], renormalization group [116–119], and effective potential [120–122] approaches, leading to an upper bound of $m_h \lesssim 135$ GeV [113]. The consistency of this bound with precision electroweak fits is a considerable success of supersymmetry. At the same time, though, one might expect that the current lower bound $m_h > 113.5$ GeV from direct Higgs searches [123–126] and the success of precision electroweak fits to the SM disfavors the possibility of light superpartners.

However, closer analysis shows that light superpartners are consistent with the current Higgs mass bound. For example, in general scenarios, the current Higgs mass limit may be satisfied with large masses only for the top and bottom squarks. Even for these, the constraints are not severe. Charginos, neutralinos, and sleptons may be light and within the reach of linear colliders. In simpler frameworks, the Higgs limit is more constraining. Even in minimal supergravity, however, the current Higgs mass bound, along with the requirement of a suitable dark matter candidate, may be satisfied either for chargino masses above 200 GeV [127] or for large m_0 [46,128]. In the latter case, charginos may be as light as their current LEP bound. The Higgs mass bound can also be made consistent with light superpartners if there are large CP-violating phases, which must necessarily cancel to high accuracy in electric dipole moments, or new singlets [129]. Thus, the current Higgs mass constraint, although already rather stringent, does not exclude the possibility of light superpartners.

The supersymmetric spectrum is also constrained by precision electroweak measurements. The effects of supersymmetry have been studied in numerous recent works (see, *e.g.*, [130–135]). While there are at present no strong indications for supersymmetry from these considerations, light superparticles cannot be excluded either. This issue is discussed further in Chapter 8, Section 3.2.

2.4 Evidence for new physics

Finally, weak-scale supersymmetry has implications for a broad range of experiments in particle physics and astrophysics. If deviations from SM predictions are found, these deviations may also constrain the scale of superpartner masses.

As an example, we consider the recently reported 2.6σ deviation in the anomalous magnetic moment of the muon [136]: $a_\mu^{\rm exp} - a_\mu^{\rm SM} = (43 \pm 16) \times 10^{-10}$. Supersymmetric contributions to a_μ are well known [137–141], and the measured deviation is naturally explained by supersymmetry [142–153]. If a supersymmetric interpretation is adopted, the result restricts the masses of some superpartners. Highly model-independent upper bounds on the mass of the lightest observable supersymmetric

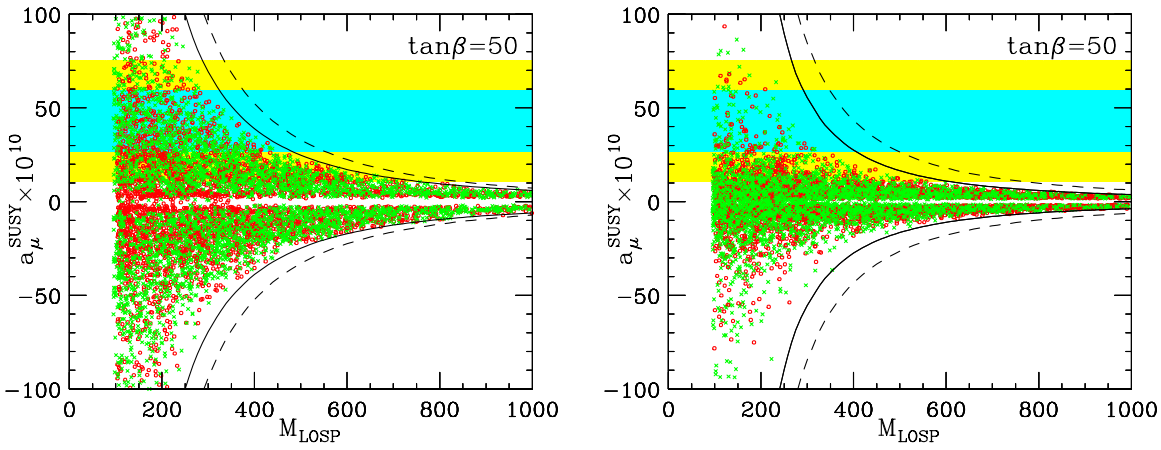

Figure 4.2: Possible values of the mass of the lightest observable supersymmetric particle, $M_{\rm LOSP}$, and the supersymmetric contribution to the muon's anomalous magnetic moment, $a_\mu^{\rm SUSY}$, assuming a stable LSP (left) and a visibly decaying LSP (right). Crosses (circles) have smuon (chargino/neutralino) LOSPs and satisfy the parameter constraints $M_2 = 2M_1$, $A_\mu = 0$, and $\tan\beta = 50$. Relaxing the gaugino unification assumption leads to the solid envelope curve, and further allowing arbitrary A_μ leads to the dashed curve. The envelope contours scale linearly with $\tan\beta$. The shaded regions are the 1σ and 2σ experimentally preferred regions. From [144].

particle are given in Fig. 4.2. If theory and experiment are required to agree within 1σ, at least one observable superpartner must be lighter than 490 GeV if the LSP is stable, and lighter than 410 GeV if the LSP decays visibly in the detector. If agreement only within 2σ is required, these limits weaken to 800 GeV and 640 GeV, respectively. The bounds are for the case $\tan\beta \leq 50$ and scale linearly with $\tan\beta$.

These results illustrate the power of evidence for new physics to constrain the scale of supersymmetry. Of course, many other experiments may also see supersymmetric effects. Among the areas in which great experimental progress is expected in the next few years are searches for new physics at the Tevatron, B physics (CP violation, rare decays), lepton flavor violation (μ-e conversion, $\mu \to e\gamma$, etc.), electric dipole moments, searches for dark matter (both direct and indirect), and cosmic ray physics. Pre-LHC evidence for supersymmetry is not guaranteed, but, in simple frameworks like minimal supergravity where systematic and comprehensive analyses are possible, it is very likely [95]. Strong evidence for new physics, even if indirect, will provide important additional constraints on the mass scale of supersymmetric particles.

3 Determination of masses and couplings

The usefulness of a linear collider in the study of SUSY particles lies both in the simplicity of the production process and in the fact that the electron can have a large longitudinal polarization. These features allow one to carry out accurate measurements of the masses and the quantum numbers of the particles being produced, and also to determine their gauge coupling constants in a model-independent manner [154,155]. Such measurements are crucial in understanding the nature of the processes being uncovered.

3.1 Measurement of superpartner masses

We begin our review of mass measurements by considering one particular process that illustrates the essential simplicity of the analyses. The process we will consider is selectron production,

$$e^+e^- \to \widetilde{e}^+_{L,R}\widetilde{e}^-_{L,R} \ , \tag{4.2}$$

where $\widetilde{e}^-_R$, $\widetilde{e}^-_L$ are the supersymmetry partners of the right- and left-handed electron. We assume that both selectrons decay by $\widetilde{e}_{L,R} \to e\widetilde{\chi}^0_1$. The process has a number of interesting features. The masses of the $\widetilde{e}_R$ and $\widetilde{e}_L$ can differ substantially. The combinations $\widetilde{e}^+_R\widetilde{e}^-_R$ and $\widetilde{e}^+_L\widetilde{e}^-_L$ are produced by s-channel photon and Z^0 exchange, but all four possible selectron combinations are produced by t-channel neutralino exchange. Thus, the study of this process can give information on SUSY masses, quantum numbers, and coupling constants.

In the reaction (4.2), the selectrons are produced at a fixed energy. Since they are scalars, they decay isotropically in their own frames. These distributions of the decay electrons and positrons boost to distributions in the lab that are flat in energy between the kinematic endpoints. The electrons and positrons then show box-like distributions. The maximum and minimum energies which form the edges of the box determine the masses of the $\widetilde{e}$ and the $\widetilde{\chi}^0_1$ through the relations

$$\begin{aligned} M^2_{\widetilde{e}} &= E^2_{\rm cm}\left\{\frac{E_{e,\rm max}E_{e,\rm min}}{(E_{e,\rm max}+E_{e,\rm min})^2}\right\} \\ M^2_{\widetilde{\chi}^0_1} &= M^2_{\widetilde{e}}\left\{1-2\frac{E_{e,\rm max}+E_{e,\rm min}}{E_{\rm cm}}\right\} \ . \end{aligned}$$

If several different combinations of selectrons are produced, the electron and positron energy spectra will show a superposition of several box-like distributions. Each set of endpoints gives the associated selectron masses and an independent determination of the $\widetilde{\chi}^0_1$ mass.

Figure 4.3 shows the electron and positron spectra for a particular set of MSUGRA parameters constructed for the Snowmass '96 summer study [156], assuming 50 fb^{-1} of data at $\sqrt{s} = 500$ GeV [157]. The simulations use the event generator ISAJET [158].

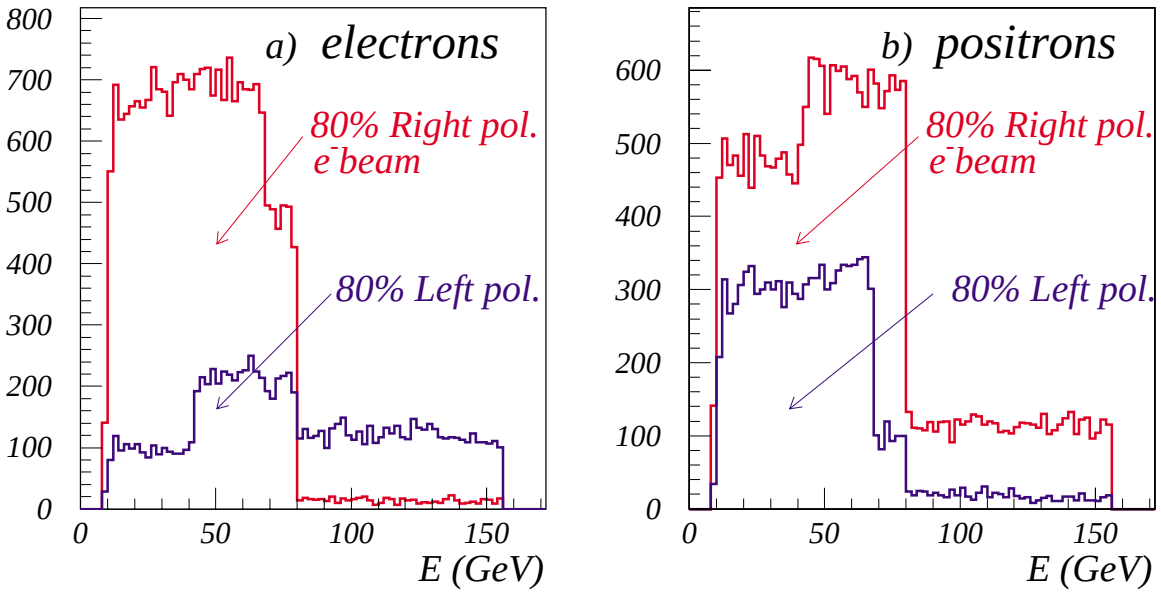

Figure 4.3: Electron and positron energy distributions for selectron pair production, with the indicated beam polarizations and integrated luminosity 50 fb^{-1} [157].

The expected box-like spectra appear clearly, with sharp endpoints. Both the electron and positron spectra have a strong dependence on polarization, and this allows us to recognize which components are associated with $\widetilde{e}_L$ and which with $\widetilde{e}_R$. The electron and positron spectra also differ from each other, reflecting the different production of $\widetilde{e}_R^-\widetilde{e}_L^+$ versus $\widetilde{e}_L^-\widetilde{e}_R^+$ from polarized beams.

Figure 4.4 compares the generated electron and positron distributions to those reconstructed using energy measurements from the electromagnetic calorimeter of the L detector described in Chapter 15. The study uses full GEANT simulation of the calorimeter [159]. The effect of resolution is clearly observed in the upper edge of the energy distribution. This analysis does not include beamstrahlung and initial state radiation, but these effects are not expected to affect significantly the determination of the edges in the energy spectra [156].

Many similar analyses of the determination of slepton masses have been carried out using fast Monte Carlo techniques [160–163]. Some of the results are summarized in Table 4.1. One can see from the table that we expect to be able to measure these masses with an accuracy of a few percent or less in most cases. The determination of the mass of the lighter chargino $\widetilde{\chi}_1^\pm$ has been studied by many groups. Measurements based on an analysis using background cuts [154,163,164] indicate that this mass can be measured with accuracies of 1% or less by this method. An interesting signal thast may be background-free is the case where one $\widetilde{\chi}_1^\pm$ decays into a lepton and a

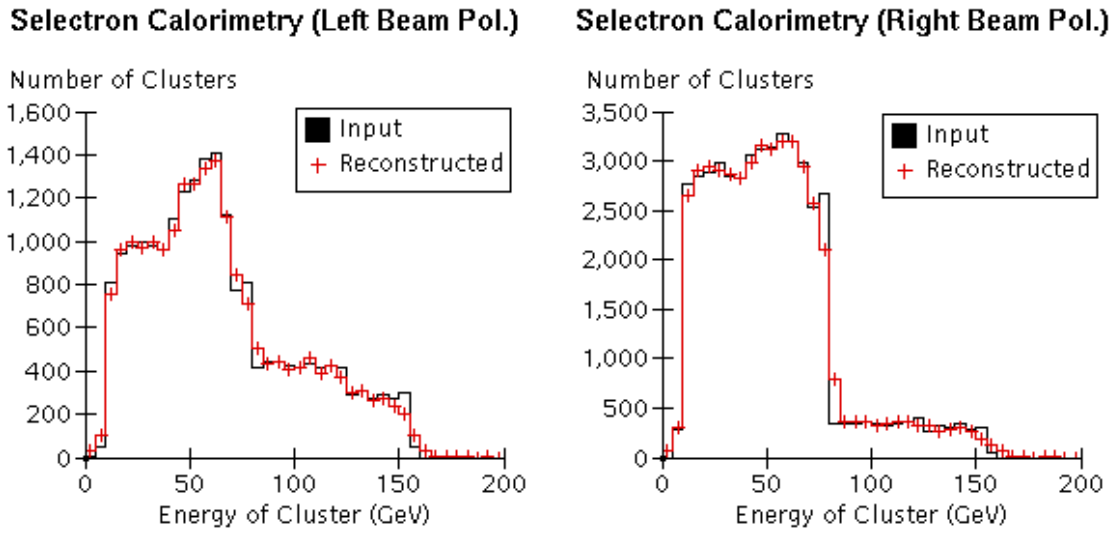

Figure 4.4: Input and calorimeter-reconstructed $e^{\pm}$ energy distributions from selectron pair production for 80% left-polarized (left) and 80% right-polarized (right) electron beams [159]. The effect of calorimeter resolution is evident at high cluster energies.

Reference	Particle	Input	Measured	Particle	Input	Measured
[157]	$\widetilde{e}_L^{\pm}$	238.2	239.4	$\widetilde{\chi}_1^0$	128.7	129.0
[157]	$\widetilde{e}_R^{\pm}$	157.0	158.0	$\widetilde{\chi}_1^0$	128.7	129.0
[173]	$\widetilde{\mu}_R^{\pm}$	157.1	143.2	$\widetilde{\chi}_1^0$	128.7	117.3
[162]	$\widetilde{\nu}_e$	206.6	199.4	$\widetilde{\chi}_1^{\pm}$	96.4	96.5
[154]	$\widetilde{\chi}_1^{\pm}$	219.0	212.0	$\widetilde{\chi}_1^0$	118.0	116.5
[165]	$\widetilde{\chi}_1^{\pm}$	238.0	239.8	$\overline{\widetilde{\nu}}_{\ell}$	220.0	221.2
[163]	$\widetilde{\chi}_2^{\pm}$	175.2	176.5	$\widetilde{\chi}_1^{\pm}$	85.9	86.1
[166]	$\widetilde{\chi}_2^{\pm}$	290.4	282.7	$\widetilde{\chi}_1^{\pm}$	96.0	97.9

Table 4.1: Comparison of the input and measured masses (in GeV) for a few supersymmetric particles as determined from the end-point spectrum of the observed particles smeared via fast MC techniques. Most of the results are based on a 50 fb^{-1} data sample. The pair of masses in each row are determined from the end-point measurement in pair-production of the first particle listed.

$\overline{\widetilde{\nu}}_{\ell}$, with the $\overline{\widetilde{\nu}}_{\ell}$ decaying to a $\nu\widetilde{\chi}_1^0$, while the other $\widetilde{\chi}_1^{\pm}$ decays into $q\overline{q}\widetilde{\chi}_1^0$. In this case, it should be possible to remove the WW background completely without affecting the signal [165]. The mass measurement for the heavier chargino $\widetilde{\chi}_2^{\pm}$ has also been studied, assuming a CM energy of 750 GeV. By using the decay of the $\widetilde{\chi}_2^{\pm}$ into $\widetilde{\chi}_1^{\pm}Z^0$, where the Z decays into leptons and the $\widetilde{\chi}_1^{\pm}$ decays into hadrons, one is able to get

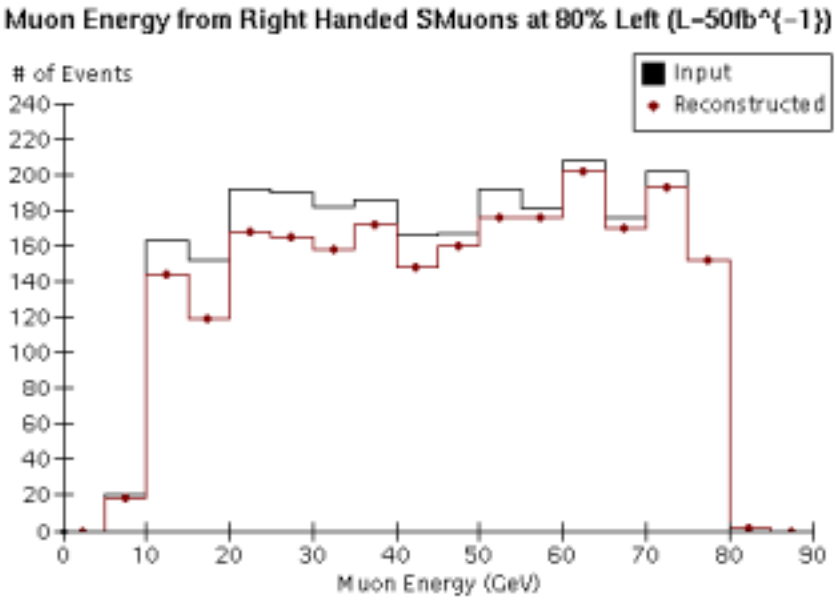

Figure 4.5: Input and tracker-reconstructed muon energy spectra from smuon pair production with an 80% left-polarized electron beam [173].

quite accurate results [166]. The conclusions of all these analyses are also shown in Table 4.1.

It is worth reviewing some of the experimental issues that arise in these measurements. We have already given an example in which the calorimeter resolution affects the mass measurements for selectrons decaying to e^- and e^+. For the case of smuons decaying to $\mu^\pm$, the corresponding issue is tracking resolution. In Fig. 4.5, we show a comparison of generator-level and reconstructed muon energy in $\widetilde{\mu}$ pair production. It is clear that the tracking reconstruction does not significantly affect the energy edge resolution, and hence it does not affect our ability to determine supersymmetric masses accurately. For chargino decays, both calorimeter and tracking resolution enter the determination of kinematic endpoints [154].

To examine the supersymmetry signals, it is necessary to remove backgrounds events efficiently. The major sources of SM backgrounds are the two-photon ($\gamma^\star\gamma^\star$) process, which gives rise to lepton and quark pairs in the detector, e^+e^- annihilation to the W^+W^-, Z^0Z^0, and Z^0h^0, and single-W production ($e\gamma^* \to \nu W$). Methods for removing the annihilation and single W backgrounds from the supersymmetry sample are explained in [154,167,168]. The two-photon background is a problem in reactions whose signatures involve missing energy, but it can be controlled by also requiring missing transverse momentum. Methods for measuring the two-photon background

have been studied in [169,168,170–172]. There may also be backgrounds from the decays of other supersymmetric particles but, in most cases, these are either small or have distinctive signals that allow one to identify them.

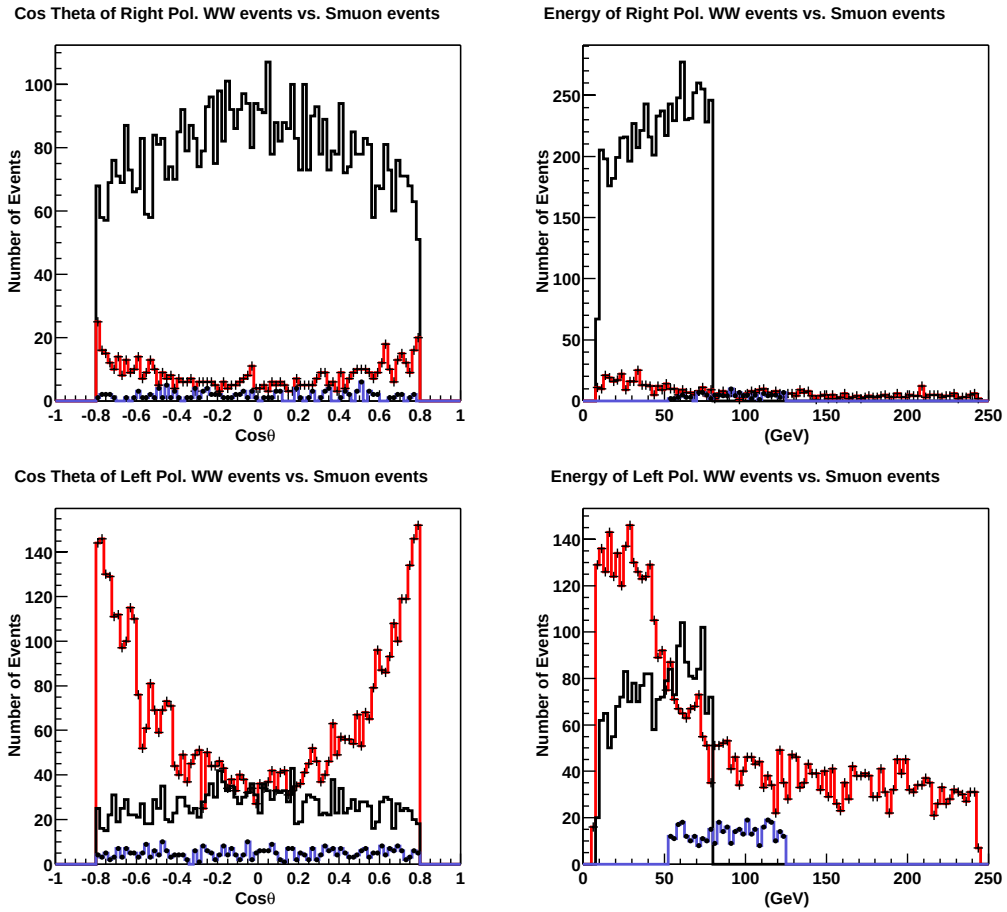

Figure 4.6: Kinematic distributions of muons from $\widetilde{\mu}_R$ pair production (solid), $\widetilde{\mu}_L$ pair production (dotted), and W^+W^- background (crossed) [173]. An electron beam polarization of 80% is assumed.

One case in which W pair production is a serious background is the study of the muon energy spectrum $\widetilde{\mu}^{\pm}_{R,L}$. The cross section for $\widetilde{\mu}$ pair production is small, and the W pair production process leads to muon pairs with missing transverse momentum from neutrinos. Figure 4.6 shows the effect of the W pair background after appropriate cuts [173]. The figure also shows that electron polarization can be used to remove this background. The $\widetilde{\mu}_R$ signal is most clearly seen with a right-handed polarized electron beam, since the W^+W^- production is strongly reduced in this case. Observing the signal for $\widetilde{\mu}_L$ is difficult with either polarization. If the model parameters are

such that the $\widetilde{\ell}_{R,L}$ is heavier than the $\widetilde{\chi}_2^0$, this problem can be avoided by studying the decay $\widetilde{\ell}_{R,L}^{\pm} \rightarrow \ell^{\pm} + \widetilde{\chi}_2^0$, with the $\widetilde{\chi}_2^0$ decaying to a lepton pair and $\widetilde{\chi}_1^0$. Then, because of the large lepton multiplicity, there are no important SM backgrounds [174].

Another kinematic method for determining the masses of supersymmetric particles is to exploit the correlations between the products of the two decaying sparticles in a given event [175]. This technique is especially useful in cases where low-p_T backgrounds tend to overwhelm the signal. Some experimental analyses have been carried out using this method [176,177], and it should receive more attention.

One can also carry out mass measurements using threshold scans [174,164], though in some cases this requires 100 fb^{-1} of luminosity per threshold. The method has the potential to measure masses with accuracies of 0.1%. The effect of backgrounds from SM processes and other SUSY signals and the effects of beamstrahlung and bremsstrahlung need to be understood to determine the systematics limits of this method [178].

A special case of spectrum parameters for which SUSY detection and mass measurement are especially difficult is that of an almost-degenerate chargino and neutralino. This situation can occur in the Higgsino limit of gaugino-Higgsino mixing, and in anomaly-mediated supersymmetry breaking (AMSB). A recent analysis [179] shows how to extract the chargino signal in this limit using the reaction $e^+e^- \rightarrow \gamma\widetilde{\chi}_1^+\widetilde{\chi}_1^-$. In some cases, in particular, those from AMSB, the $\widetilde{\chi}_1^{\pm}$ has a long enough lifetime that, at the linear collider, one can see the chargino's track in the vertex detector before it decays. One then observes a stiff track turning into a very soft track, which would be a dramatic signal.

Table 4.1 makes clear that it is possible to measure the first-generation slepton masses with a precision of about 1%. This would allow experiments at linear colliders to probe the underlying GUT-scale universality of intra-generation slepton masses, with enough sensitivity to discriminate the MSUGRA framework from other models (*e.g.*, gaugino-mediation) where small GUT-scale splittings of sleptons are expected [180]. Another important observation from Table 4.1 is that the linear collider measurements of SUSY particles will provide multiple high-accuracy measurements of the mass of the lightest neutralino $\widetilde{\chi}_1^0$. As we will discuss in Section 7, this information will directly complement supersymmetry measurements at the LHC, since this key parameter will not be well determined there.

3.2 Measurement of supersymmetry parameters

Once superpartners are identified and their masses are measured, it is important to convert the mass and cross section information into determinations of the parameters of the SUSY theory. For the example of the MSSM with R-parity conservation, studies have been done to determine how well one can measure the fundamental parameters. By studying the production and subsequent decays of $\widetilde{\chi}_1^{\pm}$ and $\widetilde{\chi}_2^{\pm}$, the masses and

the gaugino-higgsino mixing angles of these states can be measured and hence the values of the MSSM parameters M_2, μ, and tanβ can be determined to about 1% accuracy [155,181,182]. This is illustrated in Fig. 4.7, where it is shown that the value of the chargino production cross section from a right-handed polarized beam allows one to map out whether the lighter chargino is mainly gaugino or Higgsino. A measurement of both the cross section and the angular distribution allows one to measure all of the terms in the chargino mass matrix. It should be noted that the figure shows the tree-level cross section. A true determination of parameters to 1% accuracy should take account of electroweak and SUSY radiative corrections.

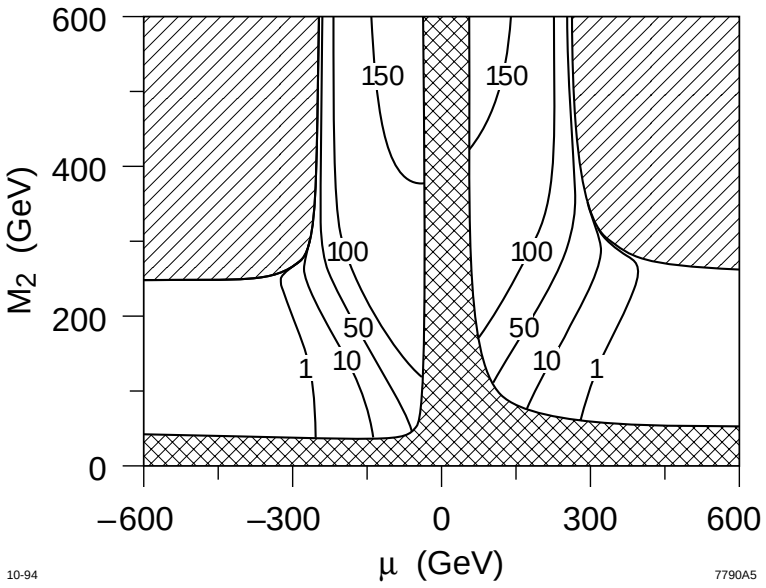

Figure 4.7: The dependence of the chargino production cross section $\sigma(e^-_R e^+ \to \widetilde{\chi}^+_1 \widetilde{\chi}^-_1)$, in fb, on M_2 and μ [155]. The value $\tan\beta = 4$ is used for this plot, but the result is only weakly dependent on this parameter.

Another method for determining whether the lightest neutralinos and chargino are mostly gaugino or Higgsino is to study slepton pair production with left-handed and right-handed beam polarization. This is done by measuring the magnitude of the cross section and the shape of the production angular distribution [154]. Similarly, measuring the cross sections of $\widetilde{t}_1$, $\widetilde{t}_2$, $\widetilde{\tau}^{\pm}_1$ and $\widetilde{\tau}^{\pm}_2$ and $\overline{\nu}_\tau$ with polarized beams allows one to determine their mixing angles [183–185]. Additional measurements associated with polarization in $\widetilde{\tau}$ reactions are discussed in [154,186].

By looking at the angular distributions of supersymmetric particles that have a t-channel exchange involving another supersymmetric particle, the mass of the exchanged particle can be determined. Similarly, if the decays of the charginos have

three-body decays because the two-body decay to $W\widetilde{\chi}_1^0$ is not allowed kinematically, decays via W^* can interfere with decays involving a virtual slepton or squark. This could give useful indirect signals for these particles in the cases where they cannot be produced because they are too heavy [187].

We should recall that the parameter $\tan\beta$ can be determined not only from supersymmetry reactions but also by direct experimental studies of the extended Higgs sector. For $\tan\beta < 30$, one can obtain an accurate value of this parameter by measuring the branching ratios for the various possible decays of the SUSY Higgs particles: H^- into $\tau\nu$, $b\overline{t}$, and W^-h, and A^0 and H^0 into $\tau^+\tau^-$, $b\overline{b}$, $t\overline{t}$, and Zh [188,189]. If the Higgs sector is heavy enough, one can include decays into lighter supersymmetric particles. These can provide quite sensitive measurements in the high-tanβ region [189].

Finally, it is important to verify the spin of each supersymmetric partner experimentally. This can be done at a linear collider, because the simplicity of the production reactions often makes the spin obvious from the angular distributions. For example, the $\widetilde{\mu}_R$ signal in Fig. 4.6 exhibits a $\sin^2\theta$ distribution that is a clear indication that the spin of the $\widetilde{\mu}_R$ is 0. The spin of supersymmetric particles can also be determined by measuring the pair-production cross section near threshold, which rises as β and β^3, where β is the particle velocity, for spin-$\frac{1}{2}$ and spin-0 particles, respectively.

4 Tests of supersymmetry

If new particles are discovered with quantum numbers expected in supersymmetry, it is desirable to determine whether they are in fact superparticles. Linear colliders can verify supersymmetry through highly model-indepedent tests accurate at the percent level. In addition, since these tests are sensitive to loop-level effects, they may yield a wealth of additional information.

Supersymmetry may be tested in many ways. For example, confirmation that some of the newly discovered particles are scalars, as discussed at the end of Section 3, constitutes an important, if weak, test of supersymmetry. More quantitatively, verification of the consistency of direct discoveries with the expected indirect supersymmetric effects in SM processes, as discussed in Chapter 8, Section 3, also provides a test of supersymmetric interpretations of new physics. Measurements of the mass differences between scalar partners in the same SU(2) doublet may also provide quantitative and rather model-independent checks.

In this section we focus on investigations of supersymmetric coupling relations, which are among the most incisive and model-independent tests. In addition to providing precise quantitative confirmation of supersymmetry, such tests may also shed light on otherwise inaccessible superpartners, much as current precision electroweak measurements bound the Higgs boson mass and constrain new physics.

4.1 Confirming supersymmetry

If supersymmetry were an exact symmetry of nature, the properties of supersymmetric particles would be completely determined by the properties of their SM partners. Of course, relations between masses are broken by soft supersymmetry breaking parameters. However, supersymmetry also predicts the equivalence of *dimensionless* couplings. For example, supersymmetry implies

$$g_i = h_i \ , \tag{4.3}$$

where g_i are the SM gauge couplings, h_i are their supersymmetric analogues, the gaugino-fermion-sfermion couplings, and the subscript $i = 1, 2, 3$ refers to the U(1), SU(2), and SU(3) gauge groups, respectively. These identities are not broken by soft supersymmetry-breaking parameters at tree level and are therefore known as "hard supersymmetry relations" [190]. They are valid in all supersymmetric theories, in contrast to other predictions such as the universality of scalar or gaugino masses. Hard supersymmetry relations therefore provide, in principle, a model-independent method of quantitatively confirming that newly-discovered particles are indeed superpartners [155,183].

4.2 Super-oblique corrections

At the loop-level, however, even hard supersymmetry relations receive corrections that would vanish in the supersymmetric limit [191]. These corrections are analogous to the oblique corrections [192] of the Standard Model. In the SM, SU(2) multiplets with custodial SU(2)-breaking masses, such as the (t, b) multiplet, induce splittings in the couplings of the (W, Z) vector multiplet at the quantum level. Similarly, in supersymmetric models, supermultiplets with soft supersymmetry-breaking masses, such as the $(\tilde{f}, f)$ supermultiplets, induce splittings in the couplings of the (gauge boson, gaugino) vector supermultiplet at the quantum level. This analogy can be made very precise [193–196]. Corrections to hard supersymmetry relations are therefore called 'super-oblique corrections', and the splittings are typically written in terms of 'super-oblique parameters.'

If some scalar superpartners $\tilde{f}$ have masses at a high scale M, and all others are light with mass $m \sim M_{\text{weak}}$, the super-oblique parameters are given by

$$\widetilde{U}_i \equiv \frac{h_i(m)}{g_i(m)} - 1 \approx \frac{g_i^2(m)}{16\pi^2} \Delta b_i \ln \frac{M}{m} \ , \tag{4.4}$$

where Δb_i is the one-loop β-function coefficient contribution from all light particles whose superpartners are heavy. Equation (4.4) is the leading logarithm contribution to $\widetilde{U}_i$. The super-oblique parameters for some representative models are given in Table 4.2. The super-oblique parameters may also receive contributions from split exotic supermultiplets, such as the messengers of gauge-mediation [193,196].

	$\widetilde{U}_1$	$\widetilde{U}_2$	$\widetilde{U}_3$
2–1 Models	$0.35\% \times \ln(M/m)$	$0.71\% \times \ln(M/m)$	$2.5\% \times \ln(M/m)$
Heavy QCD Models	$0.29\% \times \ln(M/m)$	$0.80\% \times \ln(M/m)$	—

Table 4.2: The super-oblique parameters $\widetilde{U}_i$ in two representative models: '2–1 Models,' with all first and second generation sfermions at the heavy scale M, and 'Heavy QCD Models,' with all squarks and gluinos at the heavy scale.

From Eq. (4.4) we see that, although super-oblique parameters are one-loop effects, they may be greatly enhanced if many states are heavy (large Δb_i). They also grow logarithmically with M/m: super-oblique parameters are *non-decoupling*, and so are sensitive to particles with arbitrarily high mass. As noted in Section 2, the squarks and sleptons of the first and second generations are only loosely bounded by fine-tuning arguments. They may have masses far beyond the reach of the LHC, and in fact, such massive squarks and sleptons considerably ameliorate many supersymmetric flavor and CP problems. In these cases, the super-oblique parameters are large and provide a rare window on these heavy scalars.

4.3 Measurements at linear colliders

With respect to super-oblique parameters, the program at a linear collider consists of two parts: First, one would like to verify as many hard supersymmetry relations as possible to determine that newly-discovered particles are in fact superparticles. Second, if new particles are determined to be supersymmetric, small violations of hard supersymmetry relations may provide the first evidence for as-yet-undiscovered superparticles. Precise measurements of the super-oblique parameters may constrain the mass scales of these superparticles.

The experimental observables that are dependent on super-oblique parameters have been exhaustively categorized in [194] for both lepton and hadron colliders. The most promising observables at colliders are cross sections and branching ratios involving gauginos, and several of these possibilities have been examined in detailed studies. The potential of linear colliders is, of course, highly dependent on the supersymmetry scenario realized in nature, but we present a brief synopsis below.

To date, all studies have used tree-level formulae in which the gaugino couplings are allowed to vary. Constraints on these gaugino couplings are then interpreted as measurements of super-oblique parameters. At the level of precision required, however, it will ultimately be necessary to make a detailed comparison of cross sections and other observables with full one-loop predictions. In chargino pair production, for example, studies of triangle [197–199] and box [200] contributions have been shown to be important. In addition, beam polarization may enhance the effect of quantum

corrections [198]. To extract the non-decoupling effects of very heavy superpartners, one must therefore control many other effects, including all other virtual effects, either by including data from direct detection, or by verifying that such effects are sufficiently suppressed to be negligible. The study of super-oblique parameters should be viewed as the first step in the complete program of one-loop SUSY studies that will be possible at a linear collider.

Potential super-oblique parameter measurements at a linear collider should include:

- *Measurements of* $\widetilde{U}_1$. Selectron pair production at electron colliders includes a contribution from t-channel gaugino exchange. In particular, in the reaction $e^+e^- \to \tilde{e}_R^+\tilde{e}_R^-$, its dependence upon the $\tilde{B}e\tilde{e}$ coupling h_1 has been studied in [183]. Under the assumption that the selectrons decay through $\tilde{e} \to e\tilde{B}$, the selectron and gaugino masses may be measured through kinematic endpoints. Combining this information with measurements of the differential cross section, $\widetilde{U}_1$ may be determined to $\sim 1\%$ with 20 fb^{-1} of data at $\sqrt{s} = 500$ GeV.

  This high-precision measurement may be further improved by considering the process $e^-e^- \to \tilde{e}_R^-\tilde{e}_R^-$. This process is made possible by the Majorana nature of gauginos. Relative to the e^+e^- process, this reaction benefits from large statistics for typical supersymmetry parameters and extremely low backgrounds, especially if the electron beams are right-polarized. Depending on experimental systematic errors, determinations of $\widetilde{U}_1$ at the level of 0.3% may be possible with integrated luminosities of 50 fb^{-1} [194].

- *Measurements of* $\widetilde{U}_2$. Chargino pair production has a dependence on $\widetilde{U}_2$ at lepton colliders through the $\tilde{\nu}$ exchange amplitude. This process was first studied as a way to verify hard supersymmetry relations [155]. In [194], estimates of 2–3% uncertainties for $\widetilde{U}_2$ were obtained from pair production of 172 GeV charginos with $\sqrt{s} = 400$–500 GeV. These results are conservative, and are improved in most other regions of parameter space [197]. Dramatic improvements may also be possible if both charginos are within kinematic reach and large luminosities with polarized beams are available, a scenario studied in [201].

  The process $e^+e^- \to \tilde{\nu}_e\overline{\tilde{\nu}_e}$ also depends on $\widetilde{U}_2$ through the t-channel chargino exchange amplitude. With a data sample of 100 fb^{-1}, $\widetilde{U}_2$ may be determined to $\sim 0.6\%$ [195].

- *Measurements of* $\widetilde{U}_3$. The strong super-oblique parameter may be measured through processes involving squarks. The squark pair-production cross sections at lepton colliders are independent of super-oblique corrections, but the three-body production processes, such as $\tilde{t}t\tilde{g}$ and $\tilde{b}b\tilde{g}$, have been suggested as a probe [194,196].

Squark branching ratios are also sensitive to super-oblique corrections if there are two or more competing modes [190]. In [194], parameters were studied in which the two decays $\tilde{b}_L \to b\tilde{g}$ and $\tilde{b}_L \to b\tilde{W}$ were open. For parameters where the gluino decay is suppressed by phase space, these modes may be competitive, and measurements of the branching ratios yield constraints on $\widetilde{U}_3$. For example, for $m_{\tilde{b}_L} = 300$ GeV, $\tilde{b}_L$ pair production at a $\sqrt{s} = 1$ TeV collider with integrated luminosity 200 fb^{-1} yields measurements of $\widetilde{U}_3$ at or below the 5% level for 10 GeV $\lesssim m_{\tilde{b}_L} - m_{\tilde{g}} \lesssim 100$ GeV. These measurements are typically numerically less stringent than those discussed above, but the SU(3) super-oblique correction is also larger by a factor α_s/α_w.

- *Measurements of Wino-Higgsino mixing.* The presence of the W boson mass in the tree-level chargino mixing matrix is also a consequence of supersymmetry (relating the WWh and $\tilde{W}\tilde{h}h$ couplings). Wino-Higgsino mixing receives non-decoupling corrections, and may be constrained through chargino pair production [155,197].

- *Measurements of trilinear gaugino/gauge boson couplings.* Finally, the supersymmetric equivalence of triple gauge boson and gaugino couplings may also be broken. In [202], splittings of the $WW\gamma$ and $W\tilde{W}\tilde{\gamma}$ couplings were calculated and found to be present at the few-percent level. Such splittings could be probed in $\tilde{W} \to W\tilde{\gamma}$ decays.

These studies demonstrate the promise of linear colliders for loop-level studies of supersymmetry. If charginos or sleptons are produced at linear colliders, precision tests will be able to verify that their couplings are as predicted by supersymmetry to the percent level. In addition, small corrections to these relations are sensitive to arbitrarily heavy superpartners, and, if some superpartners are kinematically inaccessible, precise determination of the super-oblique parameters may provide a target mass range for future searches.

5 Symmetry violating phenomena

5.1 R-parity violation

Up to this point we have considered only R-parity (R_p)-conserving supersymmetric theories. R_p is a multiplicative discrete symmetry [203–206] defined for each particle to be

$$R_p = (-1)^{3B+L+2S} \tag{4.5}$$

where B is baryon number, L is lepton number, and S is the particle's spin. This symmetry is not automatic in the MSSM as it is in the SM. We now consider the possibility that the symmetry is not respected [207].

Without R_p conservation, the most general gauge-invariant and Lorentz-invariant superpotential is

$$\begin{aligned} W &= \mu H_u H_d + y^e_{ij} H_d L_j e^c_k + y^d_{jk} H_d Q_j d^c_k + y^u_{jk} H_u Q_j u^c_k \\ &\quad + \lambda_{ijk} L_i L_j e^c_k + \lambda'_{ijk} L_i Q_j d^c_k + \lambda''_{ijk} u^c_i d^c_j d^c_k + \mu_i H_u L_i. \end{aligned} \tag{4.6}$$

The λ- and λ'- terms do not respect lepton number and the λ''-terms do not respect baryon number. Proton decay is unacceptably rapid if all terms are allowed without extreme suppressions; this requires $\lambda'\lambda'' \lesssim 10^{-36}$. But, since proton decay requires both lepton and baryon number violation, it is possible to escape this constraint by forbidding *one or the other* of lepton number violation or baryon number violation. That is, the constraint on $\lambda'\lambda''$ can be accomodated by setting $\lambda' = 0$ (lepton number conservation) or $\lambda'' = 0$ (baryon number conservation). The μ_i terms also violate lepton number conservation, although these terms can be defined away at tree level.

In the next few paragraphs, we will describe the signals expected at a 500 GeV linear collider for a theory with non-zero λ as the only R_p-violating couplings. We will then reanalyze the same theory but this time with only non-zero λ' couplings, and finally with only non-zero λ'' couplings. We further assume that the R_p-violating couplings are too weak to participate in observables in any way except to allow the lightest neutralino to decay promptly in the detector. Making the couplings stronger usually implies even more phenomena by which to discover supersymmetry (additional production modes via R_p violation). Making the couplings very weak will cause the phenomenology to asymptotically approach that of the MSSM with R_p conservation.

When applicable, we will illustrate phenomena with model E of [208], which is the heaviest superpartner model considered in this paper. This model assumes $M_2 = 2M_1 = 200$ GeV, $\mu = -250$ GeV, $\tan\beta = 20$, and $m_{\tilde{e}_L} = m_{\tilde{e}_R} = 200$ GeV. The chargino masses are then 173.4 and 292.1 GeV, and the neutralino masses are $97.7, 173.6, 260.8$, and 290.1 GeV.

5.1.1 $\lambda_{LLe^c} \neq 0$

In these theories the LSP always decays into two charged leptons and a neutrino (missing energy):

$$\tilde{\chi}^0_1 \to \ell^+ + \ell^- + \not{E}. \tag{4.7}$$

When superpartners are produced in pairs, they will cascade-decay down to two LSPs (plus SM jets or leptons), and the LSPs will then decay into two leptons plus missing energy. Therefore, the signal always includes at least four leptons plus missing energy, and quite often contains more leptons and additional jets from the cascades. This is a spectacular signature that will not go unnoticed. For example, the cross section for the $4l + \not{E}_T$ signature for our considered example model is approximately 274 fb, much higher than the expected 0.4 fb background rate [208].

5.1.2 $\lambda'_{LQd^c} \neq 0$

In these theories the LSP always decays into two jets with an accompanying charged lepton or neutrino:

$$\tilde{\chi}_1^0 \to l^{\pm} q\overline{q}' \quad \text{or} \quad \nu q\overline{q}. \tag{4.8}$$

All supersymmetry signals must pass through $\tilde{\chi}_1^0\tilde{\chi}_1^0 + X_{\rm SM}$, where $X_{\rm SM}$ represents SM states (jets, leptons, or neutrinos) arising from the cascade decays of the produced parent superpartners. In this case the final-state signatures of all superpartner production processes will be

$$(0, 1, \text{ or } 2 \text{ leptons}) + 4\,\text{jets} + X_{SM}. \tag{4.9}$$

Furthermore, all events that do not have 2 leptons will have some missing energy in them from escaping neutrinos.

Many of the signal events of this type of R_p violation will be swamped by backgrounds. The two most promising modes to search are $3l$ and $4l$ final states, where at least one additional lepton comes from the cascade products in $X_{\rm SM}$. Another intriguing possibility is to search for like-sign dilepton events. This signature is made possible by each independent $\tilde{\chi}_1^0$ decaying into a lepton of either positive or negative charge. Approximately one-eighth of the $\tilde{\chi}_1^0\tilde{\chi}_1^0$ decays end in like-sign dileptons. The background in this case is very small whether $X_{\rm SM}$ contains leptons or not. Furthermore, it appears that the LSP mass may be obtainable by analyzing the invariant mass distribution of the hardest lepton combined with all hadronic jets in the same hemisphere [208].

5.1.3 $\lambda''_{u^cd^cd^c} \neq 0$

In these theories the LSP always decays into three jets:

$$\tilde{\chi}_1^0 \to q' q\overline{q}. \tag{4.10}$$

All supersymmetry events will then have at least six jets from LSP decays in the final state plus the cascade decay products of the parent sparticles. Although jet reconstruction algorithms will generally not resolve all six jets, they will usually register at least three in the event [209].

Perhaps the most important signature for discovery in these theories comes from chargino pair production, where each chargino decays as $\tilde{\chi}_1^{\pm} \to l^{\pm}\nu\tilde{\chi}_1^0$. The final state will then be 2 leptons plus many jets. Unfortunately the lepton often finds itself inside one of the many hadronic jets and fails the isolation requirements. Nevertheless, the rate is sufficiently large that it is a viable signal for our example model. According to [208], the signal in this mode—including also the smaller contribution from $\tilde{\chi}_i^0\tilde{\chi}_j^0$

production—is approximately 40 fb compared to a background of 243 fb. A moderate luminosity of $10\,\mathrm{fb}^{-1}$ would produce a $S/\sqrt{B}$ significance greater than 8.

To determine the LSP mass, one can use strategies similar to ALEPH's four-jet analysis [210] to combine jets within same hemispheres to look for matching invariant mass peaks. Careful comparisons with background have not yet been performed to see how accurately the LSP mass can be extracted with this technique.

5.1.4 $\mu_i \neq 0$

The parameter space with just $\mu_i \neq 0$ is often called Bilinear R-Parity Violation ($\mathrm{BR_pV}$). It has special theoretical motivations in supersymmetry [211–214]. One interesting phenomenological feature of the model is its ability to predict the three neutrino masses and the three mixing angles by adding to the MSSM only one or two extra parameters. This is done in a SUGRA context with radiative electroweak symmetry breaking and universality of soft parameters at the GUT scale [215]. At tree level, one neutrino acquires a mass from neutrino-neutralino mixing. The masslessness and degeneracy of the other two neutrinos is lifted at one loop, giving masses and mixings that account for the solar and atmospheric neutrino anomalies [216–219]. The parameters of the model can be measured from the leptonic branching fractions of the lightest neutralino [219,220]. Thus, in this model, crucial information needed to understand neutrino physics comes from experiments at the linear collider.

5.2 Lepton flavor violation

A linear collider enables the careful study of flavor physics in supersymmetry. With the apparent confirmation of neutrino masses, non-trivial lepton-slepton flavor angles are assumed to exist. There are constraints on the magnitude of these angles from $B(\mu \to e\gamma)$ bounds, for example. However, the constraints are weaker if the sleptons are nearly degenerate in mass. We will make this assumption here, thereby invoking a super-GIM suppression to suppress the radiative flavor-violating lepton decays.

Direct production of sleptons and close scrutiny of their decays allow probing of these flavor angles at more sensitive levels [221–226]. The nearly degenerate sleptons will undergo flavor oscillation after being produced and then decay quickly. Analogous to neutrino oscillations, the detectability of slepton oscillations is best characterized in the ($\sin 2\theta$, Δm^2) plane, where θ is the angle between the weak eigenstates $|\tilde{e}\rangle$, $|\tilde{\mu}\rangle$ and the mass eigenstates $|1\rangle$, $|2\rangle$:

$$\begin{aligned} |\tilde{e}\rangle &= +\cos\theta|1\rangle + \sin\theta|2\rangle \\ |\tilde{\mu}\rangle &= -\sin\theta|1\rangle + \cos\theta|2\rangle. \end{aligned} \tag{4.11}$$

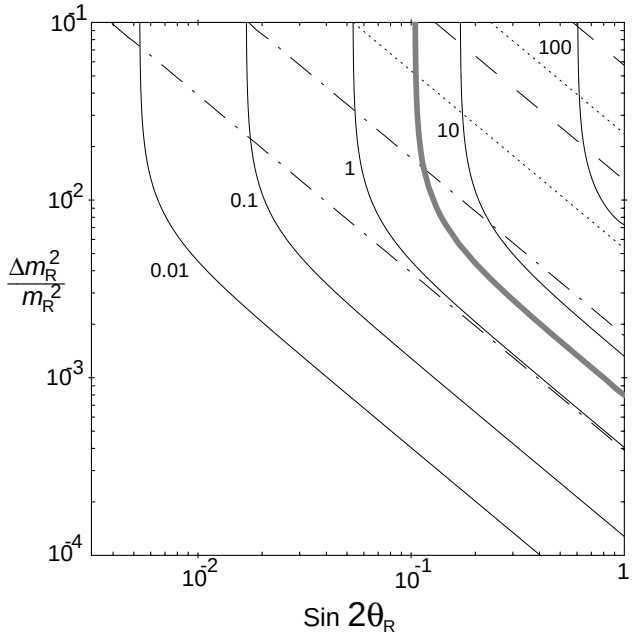

Figure 4.8: Contours of constant $\sigma(e^+e^- \to e^\pm\mu^\mp\tilde{\chi}_1^0\tilde{\chi}_1^0)$ in fb at a $\sqrt{s} = 500$ GeV $e^+e_R^-$ collider. The signal arises from right-slepton production and subsequent decay to lepton plus lightest neutralino. The $\widetilde{\ell}_R$ masses are approximately 200 GeV and the lightest neutralino is a Bino with mass 100 GeV. The thick gray contour represents optimal experimental reach with $50\,\text{fb}^{-1}$ integrated luminosity. The straight lines (dotted and dashed) represent contours of constant $B(\mu \to e\gamma)$. These depend on additional parameters such as the $\widetilde{\ell}_L$ mass and the off-diagonal entries of the slepton mass matrix. See [221] for more details.

Figure 4.8 shows contours of constant $\sigma(e^+e^- \to e^\pm\mu^\mp\tilde{\chi}_1^0\tilde{\chi}_1^0)$, in fb, at a $\sqrt{s} = 500$ GeV collider with $e^+e_R^-$ collisions. The signal arises from $\widetilde{\ell}_R$ production and subsequent decay to a lepton plus the lightest neutralino. The $\widetilde{\ell}_R$ masses are approximately 200 GeV, and the lightest neutralino is a Bino with mass 100 GeV. From this figure we can see that careful measurement of the cross section enables probing of flavor-violating couplings to very small mass splitting and mixing angle.

5.3 CP violation

The new mass parameters associated with supersymmetry may not all be real, and could lead to CP violation effects [227] at high-energy colliders. The parameters μ, M_1 and M_2 can in general be complex. By rotating the phases of the gauginos we are free to choose M_2 real, leaving us with

$$\mu = |\mu|e^{i\phi_\mu} \quad \text{and} \quad M_1 \to |M_1|e^{i\phi_1}. \tag{4.12}$$

In addition to these phases, each of the tri-scalar A terms connecting the Higgs bosons with left and right scalar superpartners of the fermions can in principle have its own independent phase.

Generic $\mathcal{O}(1)$ phases associated with superpartner masses near the weak scale are ruled out by the electric dipole moments (EDMs) of the neutron and electron if superpartners are light enough to be accessible at a 1 TeV linear collider. Therefore, we assume here that the phases must be small, $\mathcal{O}(0.1)$. We remark that tuned cancellations [228,229] may allow $\mathcal{O}(1)$ phases for light superpartners, thereby leading to effects much larger than the estimates given below.

Supersymmetric CP-violating phases have two important effects: they disrupt the relations among CP-conserving observables, and they give birth to non-zero CP-violating observables. Much work has gone into both types of analyses. For example, CP-violating observables in $e^+e^- \to t\bar{t}$ may be the most promising way to find actual CP violation effects at the linear collider. We refer the reader to [230–232] for a comprehensive review of this subject, and a description of the challenges facing experiment to confirm CP-violating effects. Here, we briefly focus on the effects that small phases have on CP-conserving observables.

Recently several groups have shown how CP-violating phases affect almost all interesting MSSM observables at a linear collider [233–235,181,236]. For example, the chargino mass eigenstates depend non-trivially on the phase of μ:

$$m^2_{\tilde{\chi}^\pm_{1,2}} = \frac{1}{2}\left[M_2^2 + |\mu|^2 + 2m_W^2 \mp \Delta_C\right], \tag{4.13}$$

where

$$\begin{aligned}\Delta_C &= \Big[(M_2^2 - |\mu|^2)^2 + 4m_W^4\cos^2 2\beta + 4m_W^2(M_2^2 + |\mu|^2) \\ &\quad + 8m_W^2 M_2|\mu|\sin 2\beta\cos\Phi_\mu\Big]^{1/2}. \end{aligned}\tag{4.14}$$

The effects of phases on observables have been illustrated in [236] with a reference model corresponding to an mSUGRA point with $m_{1/2} = 200$ GeV, $m_0 = 100$ GeV, $A_0 = 0$, $\tan\beta = 4$, and $\mu > 0$. This parameter choice corresponds to the mass values $|M_1| = 83$ GeV, $M_2 = 165$ GeV, $\mu = 310$ GeV, $m_{\tilde{e}_L} = 180$ GeV, $m_{\tilde{\nu}} = 166$ GeV, and $m_{\tilde{e}_R} = 132$ GeV. In Fig. 4.9, the effects of varying the phases ϕ_1 and ϕ_μ are demonstrated for several observables.

Motivated by the EDM constraints on the phases of supersymmetric mass parameters, the authors of [236] set $\phi_\mu = 0$ and simulated how evidence for a small but non-zero ϕ_1 phase would be extracted at a linear collider. They generated 10000 data sets, smeared with respect to the true values by experimental resolution. The input data included three cross sections ($\tilde{\chi}^0_1\tilde{\chi}^0_2$, $\tilde{\chi}^0_2\tilde{\chi}^0_2$, and $\tilde{\chi}^\pm_1\tilde{\chi}^\mp_1$) and three masses ($m_{\tilde{\chi}^0_1}$, $m_{\tilde{\chi}^0_2}$, and $m_{\tilde{\chi}^\pm_1}$). Figure 4.10 demonstrates the extraction of several different parameters, and their interdependence. For example, the bottom figures show the

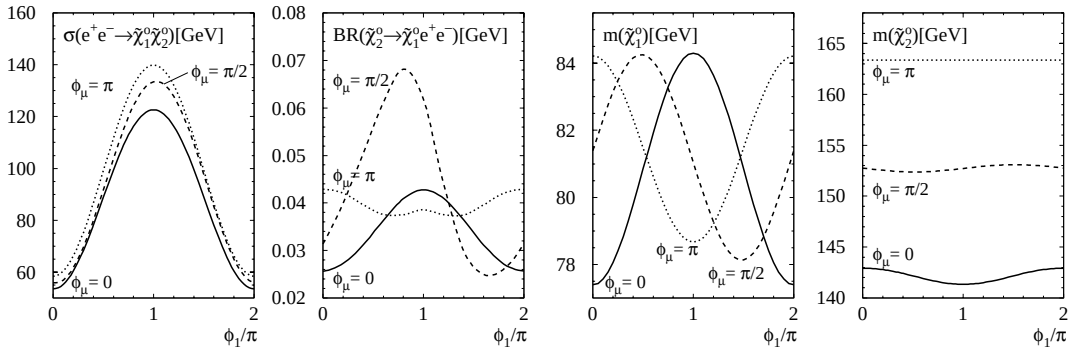

Figure 4.9: The effects on supersymmetry observables obtained by varying the phases ϕ_1 and ϕ_μ in the example model discussed in the text [236].

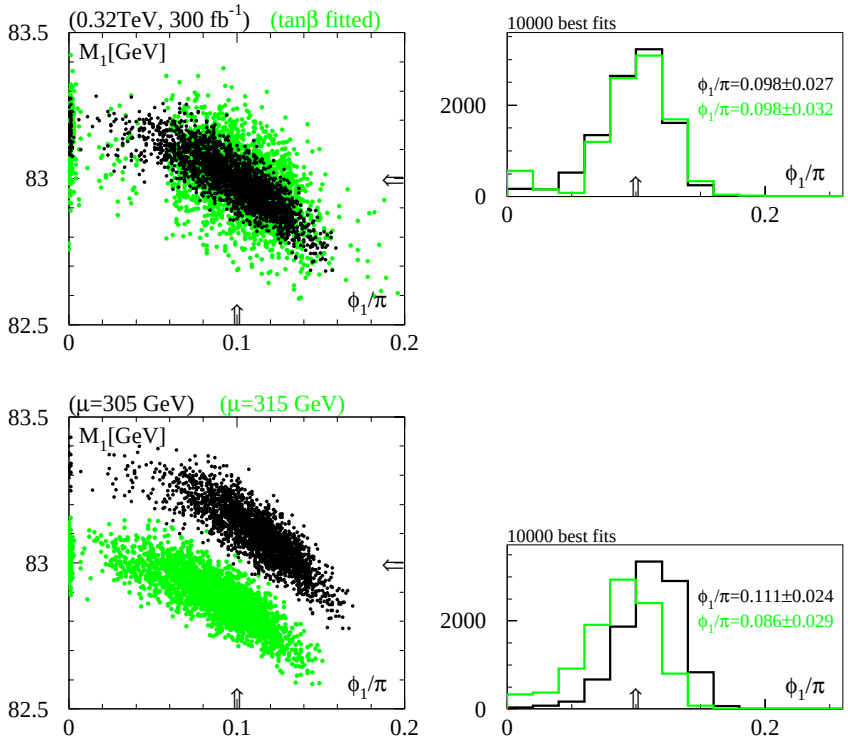

Figure 4.10: Demonstration of the interdependence of parameters in the extraction of CP-violating phases from linear collider SUSY observables [236].

systematic error one would encounter by having a wrong input for $|\mu|$ given a known $\tan\beta$. Perhaps the most interesting conclusion one can draw from this exercise is that $\phi_1 = 0$ is strongly disfavored, incicating that the linear collider measurements of CP-conserving observables can give a strong signal for nonzero CP-violating phases if they are present.

6 Supersymmetry and e^-e^-, $e^-\gamma$, and $\gamma\gamma$ colliders

6.1 Supersymmetry and e^-e^- colliders

The features of e^-e^- colliders are reviewed in Chapter 14. The unique quantum numbers of the e^-e^- initial state forbid the production of most superpartners. However, slepton pair production through t-channel neutralino exchange is always possible [237]. The opportunities at e^-e^- colliders for measurements of slepton masses, mixings, and couplings are unparalleled, and exploit many of the unique properties of e^-e^- colliders.

6.1.1 Masses

As reviewed in Section 2, masses at linear colliders are most accurately determined through kinematic endpoints and threshold scans. In e^+e^- mode, the threshold cross section for pair production of identical scalars rises as β^3, where β is the velocity of the produced particles. Threshold studies for identical scalars are therefore far less effective than for fermions, and consequently require large investments of integrated luminosity [174].

At e^-e^- colliders, however, the same-helicity selectron pair production cross section has a β dependence at threshold [238]. This is easily understood: the initial state in $e^-_R e^-_R \to \tilde{e}^-_R \tilde{e}^-_R$ has angular momentum $J = 0$, and so the selectrons may be produced in the S wave state. Cross sections for $\tilde{e}_R$ pair production in e^-e^- and e^+e^- modes are compared in Fig. 4.11. For round beams, the increased beamstrahlung and decreased luminosity of the e^-e^- mode compromise this advantage. However, beamstrahlung is reduced for flat beams [239], and mass measurements of order 100 MeV can be achieved with two orders of magnitude less luminosity than required in e^+e^- collisions [240,241]. Incidentally, the full arsenal of linear collider modes allows one to extend this mass measurement to the rest of the first-generation sleptons through a series of β threshold scans: $e^-e^- \to \tilde{e}^-_R \tilde{e}^-_R$ yields $m_{\tilde{e}_R}$; $e^+e^- \to \tilde{e}^\pm_R \tilde{e}^\mp_L$ yields $m_{\tilde{e}_L}$; $e^+e^- \to \tilde{\chi}^+_1 \tilde{\chi}^-_1$ yields $m_{\tilde{\chi}^\pm_1}$; and $e^-\gamma \to \tilde{\nu}_e \tilde{\chi}^-_1$ yields $m_{\tilde{\nu}_e}$ [242]. The process $e^-e^- \to \tilde{e}^-_R \tilde{e}^-_R$ may also be used to determine the Bino mass M_1 with high accuracy even for very large M_1 [238,241].

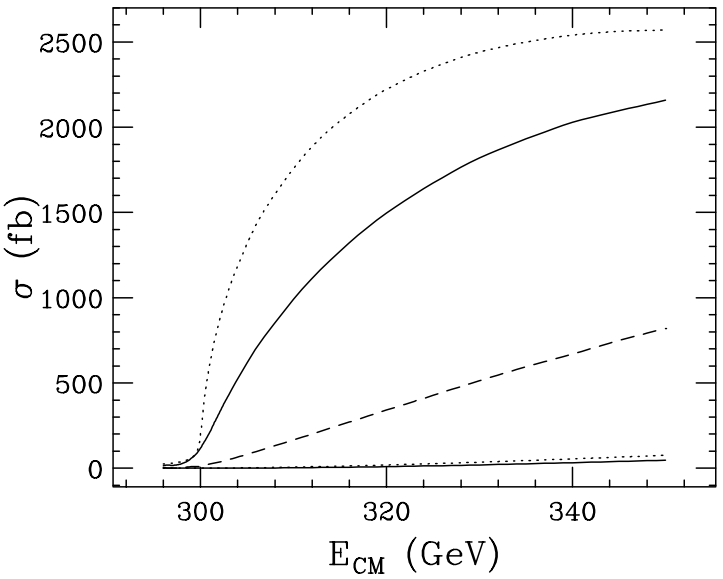

Figure 4.11: Threshold behavior for $\sigma(e^-e^- \to \tilde{e}_R^-\tilde{e}_R^-)$ (upper two contours) and $\sigma(e^+e^- \to \tilde{e}_R^+\tilde{e}_R^-)$ (lower two contours) for $m_{\tilde{e}_R} = 150$ GeV and $M_1 = 100$ GeV [240]. In each pair, the dotted curve neglects all beam effects, and the solid curve includes the initial state radiation, beamstrahlung, and beam energy spread for flat beams. Results for e^-e^- round beams (dashed) are also shown. The selectron width is included, and beam polarizations $P_{e^-} = 0.8$ and $P_{e^+} = 0$ are assumed.

6.1.2 Mixings

Now that neutrinos are known to mix, lepton flavor is no longer a perfect symmetry. Sleptons may also have inter-generational mixings. Such mixing leads to decays $\tilde{e} \to \mu\tilde{\chi}_1^0, \tau\tilde{\chi}_1^0$ and may be searched for at either e^+e^- or e^-e^- colliders.

At e^+e^- colliders, the signal is $e^+e^- \to e^\pm\mu^\mp\tilde{\chi}_1^0\tilde{\chi}_1^0,\ e^\pm\tau^\mp\tilde{\chi}_1^0\tilde{\chi}_1^0$. The backgrounds are $e^+e^- \to W^+W^-$, $e^+e^- \to \nu\nu W^+W^-$, $e^+e^- \to e^\pm\nu W^\mp$, and $\gamma\gamma \to W^+W^-$. The first two backgrounds may be reduced by e_R^- beam polarization; however, the last two are irreducible.

In the e^-e^- case, the signal is $e^-e^- \to e^-\mu^-\tilde{\chi}_1^0\tilde{\chi}_1^0,\ e^-\tau^-\tilde{\chi}_1^0\tilde{\chi}_1^0$. Among potential backgrounds, $e^-e^- \to W^-W^-$ is forbidden by total lepton number conservation, $e^-e^- \to \nu\nu W^-W^-$ and $e^-e^- \to e^-\nu W^-$ may be suppressed by right-polarizing both e^- beams, and $\gamma\gamma \to W^+W^-$ does not yield two like-sign leptons. As a result, the sensitivity of e^-e^- colliders to slepton flavor violation is much greater than at e^+e^- colliders, and probes regions of parameter space beyond current and near-future low-energy experiments searching for μ-e and τ-e transitions [221,222].

6.1.3 Couplings

The excellent properties of e^-e^- colliders are also ideal for exploring selectron gauge couplings. As noted in Section 4, precise comparisons of the $e\tilde{e}\tilde{B}$ and eeB couplings provide a model-independent test of supersymmetry. The $e\tilde{e}\tilde{B}$ coupling is a non-decoupling observable sensitive to arbitrarily heavy superpartners. The nearly background-free environment of e^-e^- colliders makes possible extremely precise measurements of selectron couplings, surpassing those available at e^+e^- colliders [194], and may help set the scale for far-future colliders in scenarios where some superpartners are extremely heavy.

6.2 Supersymmetry and $e^-\gamma$ colliders

Even if several neutralinos and charginos have light masses such that they can be produced in pairs at the LC, the sleptons might be above threshold for pair production in e^+e^- collisions. In this case, the sleptons may be accessible in the $e^-\gamma$ colliding option in the single-slepton plus lighter-neutralino final state $\tilde{\chi}_i^0\tilde{e}_{L,R}$.

This reaction was studied in [243,244,242]. For example, the parameters chosen in [242] lead to the masses: $m_{\tilde{\chi}_1^0} = 65$ GeV, $m_{\tilde{\chi}_1^\pm} = 136$ GeV, $m_{\tilde{e}_L} = 320$ GeV, $m_{\tilde{e}_R} = 307$ GeV, and $m_{\tilde{\nu}_e} = 315$ GeV. With these values, pair production of charginos is accessible at a 500 GeV linear collider but slepton pair production is not.

Figure 4.12 shows the cross sections for slepton-neutralino production as a function of the $e^-\gamma$ center-of-mass energy for the four different helicity combinations of the incoming electron and photon. The cross section for $\tilde{e}_R\tilde{\chi}_1^0$ in the $(+,+)$ helicity combination is sharply peaked at center-of-mass energies not far from the threshold. The signal for this process is e^- plus missing energy. The background [243,242] has a cross section of a few picobarns and mainly arises from $W^-\nu \to e^-\nu\nu$. This background can be reduced dramatically by using a polarized e_R^- beam. With the above parameters, using polarization and a few judicious kinematic cuts on the final state particles, the slepton can be discovered and studied. It has been estimated that both the slepton and sneutrino masses can be measured to about 1% accuracy.

6.3 Supersymmetry at $\gamma\gamma$ colliders

One of the main motivations for the $\gamma\gamma$ collider option is to study direct single Higgs production through the $\gamma\gamma h$ coupling. This motivation is especially powerful in supersymmetry since most versions of the theory predict a Higgs boson below about 135 GeV. The motivation is further strengthened by the realization that additional Higgs states exist in supersymmetry that may not be accessible at the LHC or e^+e^- annihilation but may be visible in single production from $\gamma\gamma$. These issues are discussed in more detail in Chapters 3 and 13.

For direct superpartner pair production, $\gamma\gamma$ collisions also have an important advantage: the unambiguous production mode for superpartners through photons

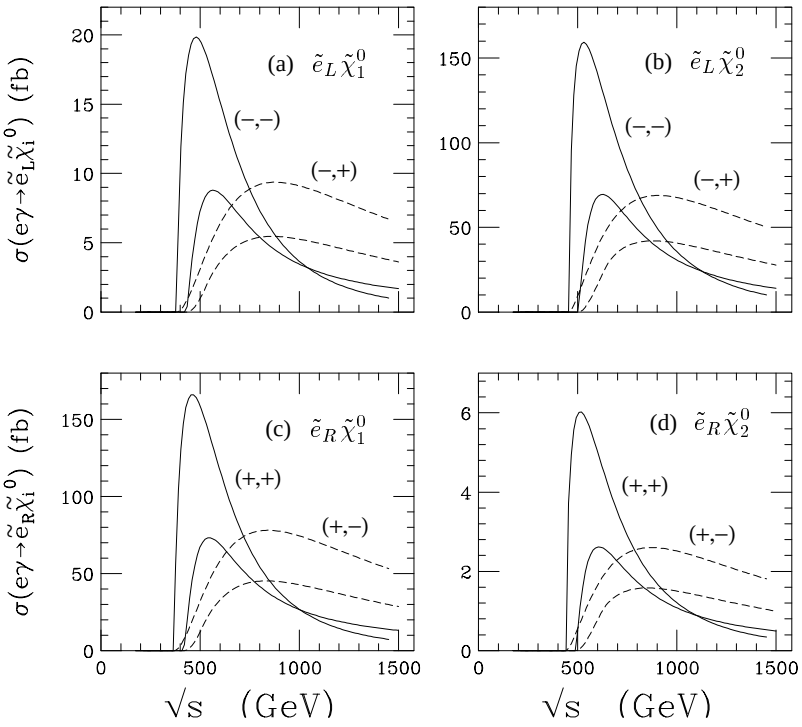

Figure 4.12: Cross sections for $e^-\gamma \to \tilde{e}\tilde{\chi}^0$ processes, from [242]. The upper two curves show the total cross section (in fb) for $e^-\gamma \to \tilde{e}\tilde{\chi}^0$ versus $\sqrt{s_{e\gamma}}$ (in GeV) for the SUSY and machine parameters given in the text: (a) $\tilde{e}_L\tilde{\chi}_1^0$; (b) $\tilde{e}_L\tilde{\chi}_2^0$; (c) $\tilde{e}_R\tilde{\chi}_1^0$; (d) $\tilde{e}_R\tilde{\chi}_2^0$. The solid curves represent e, γ helicities $(-,-)$ for (a), (b) and $(+,+)$ for (c), (d). The dashed curves represent helicities $(-,+)$ for (a), (b) and $(+,-)$ for (c), (d). The lower two curves are corresponding results, convoluted with the backscattered photon spectrum, versus $\sqrt{s_{ee}}$.

coupled to charge. Knowing exactly how a particle is produced reaps great benefits when analyzing the actual data recorded by the detectors. Production cross sections of superpartners have been calculated most recently by [245,246]. It has been argued [246] that some observables derived from $\gamma\gamma \to \chi_1^\pm\chi_1^\mp$ production are very useful in extracting fundamental parameters of the supersymmetric Lagrangian. The special advantages $\gamma\gamma$ collisions offer supersymmetry deserve additional careful study.

7 Comparison with LHC

If SUSY is relevant to electroweak symmetry breaking, then the arguments summarized in Section 2 suggest that in many models the gluino and some squark masses are less than $\mathcal{O}(1$ TeV). This is also true in most models with SUSY particles visible at a 500 GeV LC. Gluinos and squarks then dominate the LHC SUSY cross section,

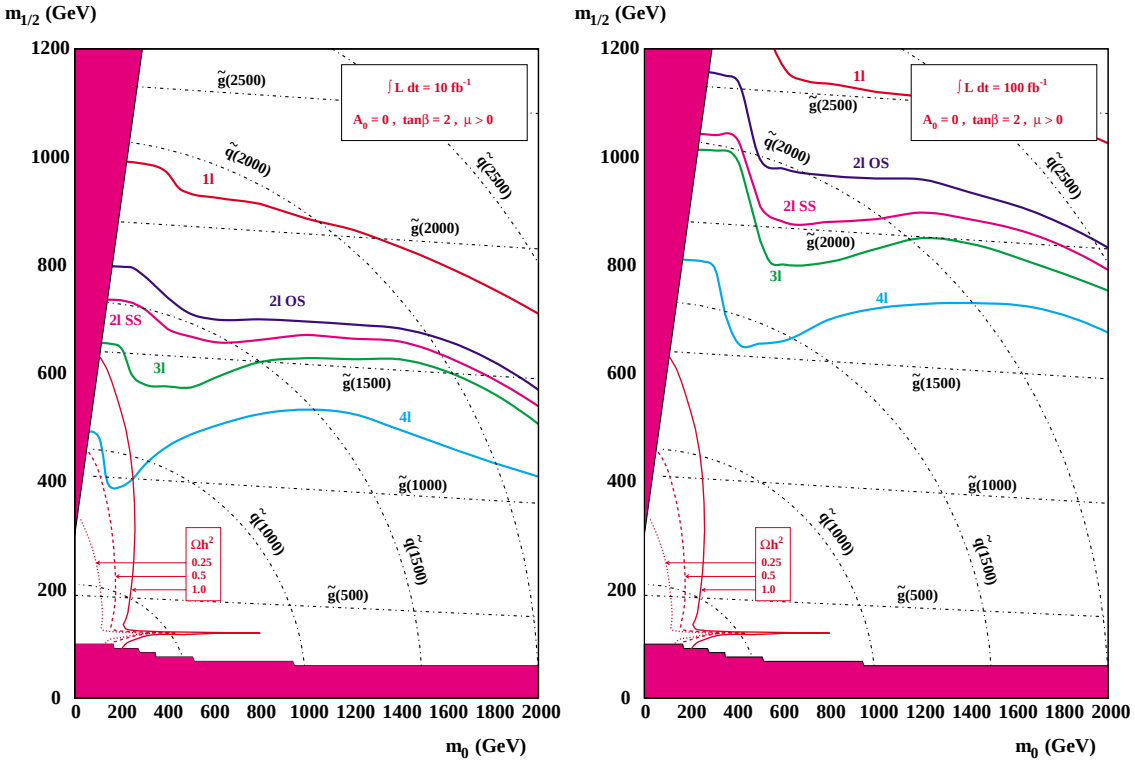

Figure 4.13: Plot of 5σ reach with multiple jets plus $\not\!\!E_T$ plus leptons in minimal SUGRA model at LHC for 10 fb^{-1} (left) and 100 fb^{-1} (right) [248]. Also shown are contours of the squark and gluino masses and of the cold dark matter density Ωh^2.

which is of order 10 pb. Since they are strongly produced, it is easy to separate SUSY from SM backgrounds provided only that the SUSY decays are distinctive. In the MSUGRA model, these decays produce multiple jets and $\not\!\!E_T$ plus varying numbers of leptons [247]. Figure 4.13 shows the 5σ reach in this model at the LHC for an integrated luminosity of 10 fb^{-1} and 100 fb^{-1} [248]. The reach is comfortably more than the expected mass range.

While the reach in Fig. 4.13 has been calculated for a specific SUSY model, the multiple jet plus $\not\!\!E_T$ signature is generic in most R-parity-conserving models. GMSB models can give additional photons or leptons or long-lived sleptons with high p_T but $\beta < 1$, making the search easier [249,250]. R-parity-violating models with leptonic $\widetilde{\chi}_1^0$ decays also give extra leptons and very likely violate e-μ universality. R-parity-violating models with $\widetilde{\chi}_1^0 \to qqq$ give signals at the LHC with very large jet multiplicity, for which the SM background is not well known. For such models, it may be necessary to rely on leptons produced in the cascade decay of the gluinos and squarks. In AMSB models, cascade decays of gluinos and squarks again lead to a substantial reach for SUSY by the LHC [251]. In all cases, it seems likely that SUSY can be

discovered at the LHC if the masses are in the expected range [252–254].

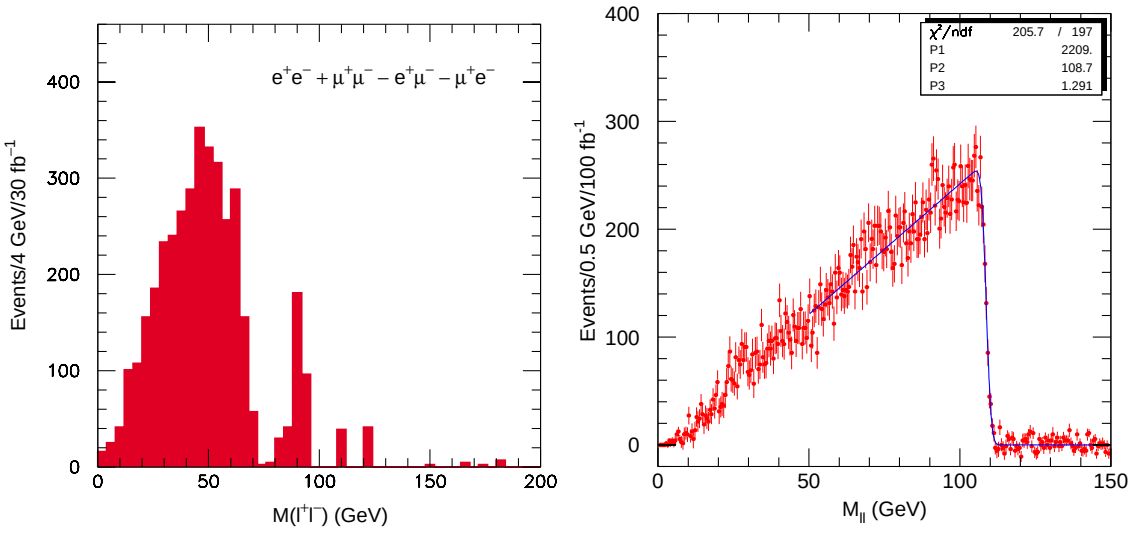

Figure 4.14: Plot of the $e^+e^- + \mu^+\mu^- - e^\pm\mu^\mp$ mass distribution for LHC SUGRA Point 4 with direct $\widetilde{\chi}_2^0 \to \widetilde{\chi}_1^0 \ell\ell$ decay (left) and for LHC SUGRA Point 5 with $\widetilde{\chi}_2^0 \to \widetilde{\ell}^\pm \ell^\mp \to \widetilde{\chi}_1^0 \ell^+ \ell^-$ (right) [252]. The event generator ISAJET is used. The shape of the peak on the left plot below 70 GeV should be compared to the shape of the peak in the right plot. The left plot also contains a $Z \to \ell^+\ell^-$ signal that comes from heavier gauginos.

The main problem at the LHC is not to observe a signal that deviates from the SM but to separate the many different channels produced by all the SUSY cascade decays from the produced squarks [255] and gluinos. One promising approach is to try to identify particular decay chains and to measure kinematic endpoints for combinations of the visible particles in these [256]. For example, the $\ell^+\ell^-$ mass distribution from $\widetilde{\chi}_2^0 \to \widetilde{\chi}_1^0 \ell^+\ell^-$ has an endpoint that measures $M_{\widetilde{\chi}_2^0} - M_{\widetilde{\chi}_1^0}$ [257], while the distribution from $\widetilde{\chi}_2^0 \to \widetilde{\ell}^\pm \ell^\mp \to \widetilde{\chi}_1^0 \ell^+ \ell^-$ has a different shape and measures

$$M_{\ell\ell}^{\max} = \sqrt{\frac{(M^2_{\widetilde{\chi}_2^0} - M^2_{\widetilde{\ell}})(M^2_{\widetilde{\ell}} - M^2_{\widetilde{\chi}_1^0})}{M^2_{\widetilde{\ell}}}} \; .$$

The flavor-subtraction combination $e^+e^- + \mu^+\mu^- - e^\pm\mu^\mp$ removes backgrounds from two independent decays. Dilepton mass distributions [252] after cuts for an example of each decay are shown in Fig. 4.14.

If a longer decay chain can be identified, then more combinations of masses can be measured. Consider, for example, the decay chain

$$\widetilde{q}_L \to \widetilde{\chi}_2^0 q \to \widetilde{\ell}_R^\pm \ell^\mp q \to \widetilde{\chi}_1^0 \ell^+ \ell^- q \; .$$

For this decay chain, kinematics gives $\ell^+\ell^-$, $\ell^+\ell q$, and two ℓq endpoints in terms of the masses. If a lower limit is imposed on the $\ell^+\ell^-$ mass, there is also a $\ell^+\ell^- q$ lower edge. With suitable cuts all of these can be measured [252,258] for the cases considered. The statistical errors on the measured endpoints are typically comparable to the systematic limits, $\mathcal{O}(0.1\%)$ for leptons and $\mathcal{O}(1\%)$ for jets. Figure 4.15 shows a scatter plot of the resulting $\widetilde{\ell}_R$ and $\widetilde{\chi}_1^0$ masses for LHC SUGRA Point 5 and for a similar point in another SUSY model with this decay chain [259]. The relations between masses are determined with good precision, so these two models are easily distinguished. However, the LSP mass is only measured to $\mathcal{O}(10\%)$.

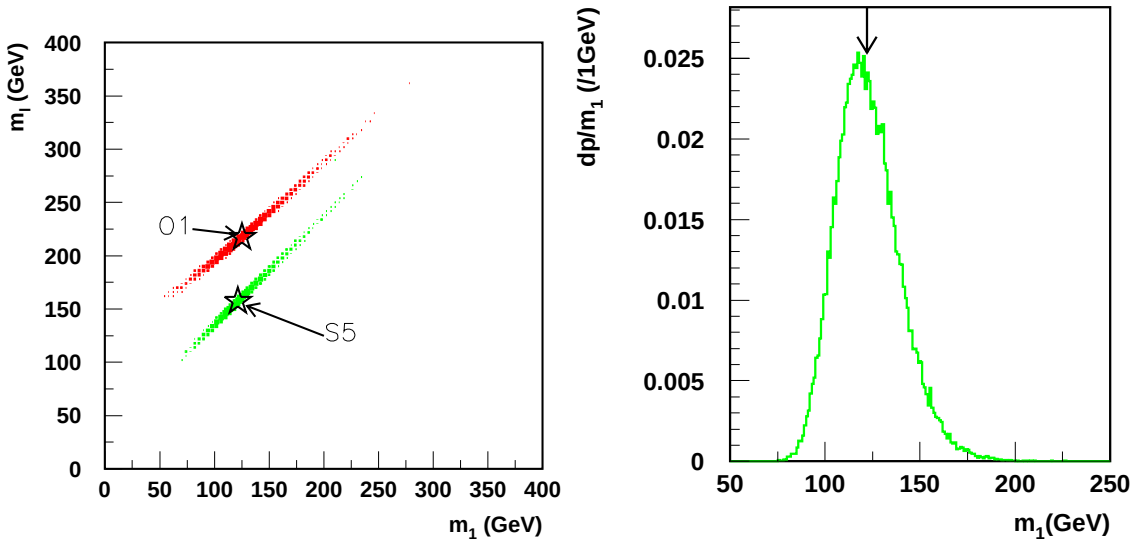

Figure 4.15: Left: Scatter plot of reconstructed values of the $\widetilde{\ell}_R$ and $\widetilde{\chi}_1^0$ masses for LHC Point 5 (S5) and for a different model (O1) using the decay chain $\widetilde{q}_L \to \widetilde{\chi}_2^0 q \to \widetilde{\ell}_R \ell q \to \widetilde{\chi}_1^0 \ell\ell q$. Right: Projection of $M_{\widetilde{\chi}_1^0}$ for LHC Point 5 [259].

Analyses such as these have proved useful for a number of SUSY points in a variety of SUSY models [252]. The method seems fairly general: there is usually at least one distinctive mode — typically $\widetilde{\chi}_2^0 \to \widetilde{\chi}_1^0 \ell^+\ell^-$, $\widetilde{\chi}_2^0 \to \widetilde{\ell}_R^\pm \ell^\mp$, or $\widetilde{\chi}_2^0 \to \widetilde{\chi}_1^0 h \to \widetilde{\chi}_1^0 b\overline{b}$ — from which to start. But some points are much more difficult than others. For example, in MSUGRA with $\tan\beta \gg 1$ it is possible to choose parameters such that the only allowed 2-body decays of $\widetilde{\chi}_2^0$ and $\widetilde{\chi}_1^\pm$ are $\widetilde{\tau}_1^\pm \tau^\mp$ and $\widetilde{\tau}_1^\pm \nu_\tau$ [260] respectively.[1] These modes then have branching ratios in excess of 99%. While it is possible to identify and to measure hadronic τ decays [252], the measurements are much less precise than those involving leptons. Even if τ decays are not dominant, they may be important, since they can provide information on $\widetilde{\tau}_L - \widetilde{\tau}_R$ and gaugino-Higgsino mixing.

[1]The simple class of such models considered in [252], however, gives an excessively large contribution to $g_\mu - 2$ [136].

If SUSY is found at the LHC, the SUSY events will contain much more information than just endpoints like those described above. For example, while it is not possible to reconstruct $\widetilde{\chi}_1^\pm$ decays in the same way because of the missing neutrino, one can get information about the chargino mass by studying $M_{\ell q}$ and other distributions for 1-lepton events. Cross sections and branching ratios can also be measured; interpretation of these will be limited by the theoretical errors on the calculation of cross sections and acceptances. Without real experimental data, it is difficult to assess such theoretical systematic errors.

SUSY signatures at the LHC typically come from a combination of many SUSY particles, so the analysis is considerably more complicated than that at a LC. However, the initial steps at the LHC are fairly clear. First, one will look for a deviation from the SM in inclusive distributions such as multiple jets plus $\not\!\!E_T$, perhaps accompanied by leptons and/or photons. If a signal consistent with SUSY is found, it should determine both the mass scale [252,261] and the qualitative nature of the signal. (As a simple example, in a GMSB model with a long-lived slepton NLSP, SUSY events would contain two high-p_T particles with $\beta < 1$.) Next, one will look for various kinematic endpoints like those described above and use them further to constrain the SUSY masses. After this, one will look at more model-dependent quantities such as kinematic distributions, cross sections, and branching ratios. These seem difficult to assess without real data.

This program is likely to provide considerable information about gluinos, squarks, and their primary decay products, including $\widetilde{\chi}_1^0$, $\widetilde{\chi}_2^0$, $\widetilde{\chi}^\pm$, and any sleptons that occur in their decays. It is more dangerous to predict what cannot be done, but there are measurements that appear difficult at the LHC and that could be done at a 500 GeV LC. For example:

- While it is possible to measure the $\widetilde{\chi}_1^0$ mass at the LHC in favorable cases, it seems difficult to reduce the error below $\mathcal{O}(10\%)$. If any visible SUSY particle is produced at a LC, the error on $M_{\widetilde{\chi}_1^0}$ should be $\mathcal{O}(1\%)$.

- Sleptons that are not produced in $\widetilde{\chi}_2^0$ or $\widetilde{\chi}_1^\pm$ decays are difficult to study at the LHC: both the Drell-Yan process and decays of heavier gauginos typically give very small rates [262]. They can be precisely measured at a LC.

- Distinguishing $\widetilde{\ell}_L$ from $\widetilde{\ell}_R$ appears very difficult at the LHC except perhaps for $\widetilde{\tau}$'s, but this is straightforward at a LC using the polarized beam.

- Hadronic τ decays are easier to identify and to measure at a LC because there is no underlying hadronic event.

- Branching ratios currently seem difficult to measure with high precision at the LHC: both the production cross sections and the acceptance have theoretical

uncertainties of $\mathcal{O}(10\%)$. In particular, it seems difficult to make precise tests of SUSY relations among couplings.

More generally, while the LHC seems sure to discover SUSY at the TeV scale if it exists, the measurements of SUSY that can be made there depend on the SUSY model. A LC can provide precise, detailed measurements of any kinematically accessible SUSY particles. Ultimately, one will want such measurements for the entire SUSY spectrum.

References

[1] The LEP Collaborations, the LEP Electroweak Working Group, and the SLD Heavy Flavour and Electroweak Working Groups, hep-ex/0103048, CERN-EP/2001-021 (February 28, 2001).

[2] L. Maiani, in *Proc. Gif-sur-Yvette Summer School* (Paris, 1980), p. 3.

[3] M. Veltman, Acta Phys. Polon. **B12**, 437 (1981).

[4] E. Witten, Nucl. Phys. **B188**, 513 (1981).

[5] R. K. Kaul, Phys. Lett. **B109**, 19 (1982).

[6] S. Dimopoulos, S. Raby and F. Wilczek, Phys. Rev. **D24**, 1681 (1981).

[7] U. Amaldi *et al.*, Phys. Rev. **D36**, 1385 (1987).

[8] P. Langacker and M. Luo, Phys. Rev. **D44**, 817 (1991).

[9] J. Bagger, K. Matchev and D. Pierce, Phys. Lett. **B348**, 443 (1995) [hep-ph/9501277].

[10] P. Langacker and N. Polonsky, Phys. Rev. **D52**, 3081 (1995) [hep-ph/9503214].

[11] H. Goldberg, Phys. Rev. Lett. **50**, 1419 (1983).

[12] C. Ahn *et al.*, High-Energy E+ E- Collider," SLAC-0329.

[13] P. M. Zerwas, editor, "E+ E- Collisions At 500-Gev: The Physics Potential. Proceedings, Workshop, Munich, Germany, February 4, 1991, Annecy, France, June 10-11, 1991, Hamburg, Germany, September 2-3, 1991," DESY-92-123A-B.

[14] JLC Group Collaboration, KEK-92-16.

[15] S. Kuhlman *et al.* [NLC ZDR Design Group and NLC Physics Working Group Collaboration], hep-ex/9605011.

[16] M. Danielson *et al.*, in *New Directions in High Energy Physics*, Proc. 1996 Snowmass Summer Study, editors D. Cassel, L. Trindle Gennari and R. H. Siemann (SLAC, 1997).

[17] S. Abdullin *et al.*, hep-ph/0005142.

[18] R. D. Heuer, D. Miller, F. Richard and P. Zerwas, DESY-01-011C.

[19] H. P. Nilles, Phys. Rept. **110** (1984) 1.

[20] H. E. Haber and G. L. Kane, Phys. Rept. **117** (1985) 75.
[21] G. F. Giudice and R. Rattazzi, Phys. Rept. **322**, 419 (1999) [hep-ph/9801271].
[22] L. Randall and R. Sundrum, Nucl. Phys. **B557**, 79 (1999) [hep-th/9810155].
[23] G. F. Giudice, M. A. Luty, H. Murayama and R. Rattazzi, JHEP **9812**, 027 (1998) [hep-ph/9810442].
[24] J. Ellis, K. Enqvist, D. V. Nanopoulos and F. Zwirner, Mod. Phys. Lett. **A1**, 57 (1986).
[25] R. Barbieri and G. F. Giudice, Nucl. Phys. **B306**, 63 (1988).
[26] G. G. Ross and R. G. Roberts, Nucl. Phys. **B377**, 571 (1992).
[27] B. de Carlos and J. A. Casas, Phys. Lett. **B309**, 320 (1993) [hep-ph/9303291].
[28] G. W. Anderson and D. J. Castaño, Phys. Lett. **B347**, 300 (1995) [hep-ph/9409419].
[29] G. W. Anderson and D. J. Castaño, Phys. Rev. **D52**, 1693 (1995) [hep-ph/9412322].
[30] G. W. Anderson and D. J. Castaño, Phys. Rev. **D53**, 2403 (1996) [hep-ph/9509212].
[31] S. Dimopoulos and G. F. Giudice, Phys. Lett. **B357**, 573 (1995) [hep-ph/9507282].
[32] A. Pomarol and D. Tommasini, Nucl. Phys. **B466**, 3 (1996) [hep-ph/9507462].
[33] K. Agashe and M. Graesser, Nucl. Phys. **B507**, 3 (1997) [hep-ph/9704206].
[34] P. Ciafaloni and A. Strumia, Nucl. Phys. **B494**, 41 (1997) [hep-ph/9611204].
[35] G. Bhattacharyya and A. Romanino, Phys. Rev. **D55**, 7015 (1997) [hep-ph/9611243].
[36] R. Barbieri and A. Strumia, Phys. Lett. **B433**, 63 (1998) [hep-ph/9801353].
[37] L. Giusti, A. Romanino and A. Strumia, Nucl. Phys. **B550**, 3 (1999) [hep-ph/9811386].
[38] A. Romanino and A. Strumia, Phys. Lett. **B487**, 165 (2000) [hep-ph/9912301].
[39] K. L. Chan, U. Chattopadhyay and P. Nath, Phys. Rev. **D58**, 096004 (1998) [hep-ph/9710473].
[40] P. H. Chankowski, J. Ellis and S. Pokorski, Phys. Lett. **B423**, 327 (1998) [hep-ph/9712234].
[41] P. H. Chankowski, J. Ellis, M. Olechowski and S. Pokorski, Nucl. Phys. **B544**, 39 (1999) [hep-ph/9808275].
[42] G. L. Kane and S. F. King, Phys. Lett. **B451**, 113 (1999) [hep-ph/9810374].
[43] M. Bastero-Gil, G. L. Kane and S. F. King, Phys. Lett. **B474**, 103 (2000) [hep-ph/9910506].
[44] J. L. Feng, K. T. Matchev and T. Moroi, Phys. Rev. Lett. **84**, 2322 (2000) [hep-ph/9908309].

[45] J. L. Feng, K. T. Matchev and T. Moroi, Phys. Rev. **D61**, 075005 (2000) [hep-ph/9909334].

[46] J. L. Feng and K. T. Matchev, Phys. Rev. **D63**, 095003 (2001) [hep-ph/0011356].

[47] M. Drees, Phys. Rev. **D33**, 1468 (1986).

[48] M. Dine, A. Kagan and S. Samuel, Phys. Lett. **B243**, 250 (1990).

[49] G. Dvali and A. Pomarol, Phys. Rev. Lett. **77**, 3728 (1996) [hep-ph/9607383].

[50] G. Dvali and A. Pomarol, Nucl. Phys. **B522**, 3 (1998) [hep-ph/9708364].

[51] A. G. Cohen, D. B. Kaplan and A. E. Nelson, Phys. Lett. **B388**, 588 (1996) [hep-ph/9607394].

[52] R. Zhang, Phys. Lett. **B402**, 101 (1997) [hep-ph/9702333].

[53] H. P. Nilles and N. Polonsky, Phys. Lett. **B412**, 69 (1997) [hep-ph/9707249].

[54] J. L. Feng, C. Kolda and N. Polonsky, Nucl. Phys. **B546**, 3 (1999) [hep-ph/9810500].

[55] J. Bagger, J. L. Feng and N. Polonsky, Nucl. Phys. **B563**, 3 (1999) [hep-ph/9905292].

[56] J. A. Bagger, J. L. Feng, N. Polonsky and R. Zhang, Phys. Lett. **B473**, 264 (2000) [hep-ph/9911255].

[57] Q. Shafi and Z. Tavartkiladze, Phys. Lett. **B473**, 272 (2000) [hep-ph/9911264].

[58] H. Baer, M. A. Díaz, P. Quintana and X. Tata, JHEP **0004**, 016 (2000) [hep-ph/0002245].

[59] H. Baer, C. Balazs, P. Mercadante, X. Tata and Y. Wang, Phys. Rev. **D63**, 015011 (2001) [hep-ph/0008061].

[60] H. Baer, C. Balazs, M. Brhlik, P. Mercadante, X. Tata and Y. Wang, hep-ph/0102156.

[61] J. Hisano, K. Kurosawa and Y. Nomura, Phys. Lett. **B445**, 316 (1999) [hep-ph/9810411].

[62] J. Hisano, K. Kurosawa and Y. Nomura, Nucl. Phys. **B584**, 3 (2000) [hep-ph/0002286].

[63] D. E. Kaplan and G. D. Kribs, Phys. Rev. **D61**, 075011 (2000) [hep-ph/9906341].

[64] J. L. Feng and T. Moroi, Phys. Rev. **D61**, 095004 (2000) [hep-ph/9907319].

[65] K. Agashe, Phys. Rev. **D61**, 115006 (2000) [hep-ph/9910497].

[66] U. Chattopadhyay, A. Datta, A. Datta, A. Datta and D. P. Roy, Phys. Lett. **B493**, 127 (2000) [hep-ph/0008228].

[67] B. C. Allanach, J. P. Hetherington, M. A. Parker and B. R. Webber, JHEP **0008**, 017 (2000) [hep-ph/0005186].

[68] U. Chattopadhyay, T. Ibrahim and D. P. Roy, hep-ph/0012337.

[69] G. F. Giudice and A. Masiero, Phys. Lett. **B206**, 480 (1988).

[70] J. Ellis, J. S. Hagelin, D. V. Nanopoulos and M. Srednicki, Phys. Lett. **B127**, 233 (1983).

[71] A. H. Jaffe *et al.*, astro-ph/0007333.

[72] K. Griest and D. Seckel, Phys. Rev. **D43**, 3191 (1991).

[73] P. Gondolo and G. Gelmini, Nucl. Phys. **B360**, 145 (1991).

[74] P. Nath and R. Arnowitt, Phys. Rev. Lett. **70**, 3696 (1993) [hep-ph/9302318].

[75] S. Mizuta and M. Yamaguchi, Phys. Lett. **B298**, 120 (1993) [hep-ph/9208251].

[76] J. Ellis, T. Falk and K. A. Olive, Phys. Lett. **B444**, 367 (1998) [hep-ph/9810360].

[77] M. E. Gomez, G. Lazarides and C. Pallis, Phys. Rev. **D61**, 123512 (2000) [hep-ph/9907261].

[78] M. Drees and M. M. Nojiri, Phys. Rev. **D47**, 376 (1993) [hep-ph/9207234].

[79] K. A. Olive and M. Srednicki, Phys. Lett. **B230**, 78 (1989).

[80] K. Griest, M. Kamionkowski and M. S. Turner, Phys. Rev. **D41**, 3565 (1990).

[81] K. A. Olive and M. Srednicki, Nucl. Phys. **B355**, 208 (1991).

[82] J. L. Lopez, K. Yuan and D. V. Nanopoulos, Phys. Lett. **B267**, 219 (1991).

[83] S. Kelley, J. L. Lopez, D. V. Nanopoulos, H. Pois and K. Yuan, Phys. Rev. **D47**, 2461 (1993) [hep-ph/9207253].

[84] R. G. Roberts and L. Roszkowski, Phys. Lett. **B309**, 329 (1993) [hep-ph/9301267].

[85] G. L. Kane, C. Kolda, L. Roszkowski and J. D. Wells, Phys. Rev. **D49**, 6173 (1994) [hep-ph/9312272].

[86] H. Baer and M. Brhlik, Phys. Rev. **D53**, 597 (1996) [hep-ph/9508321].

[87] R. Arnowitt and P. Nath, Phys. Lett. **B437**, 344 (1998) [hep-ph/9801246].

[88] S. Abdullin and F. Charles, Nucl. Phys. **B547**, 60 (1999) [hep-ph/9811402].

[89] J. Ellis, G. Ganis and K. A. Olive, Phys. Lett. **B474**, 314 (2000) [hep-ph/9912324].

[90] M. Drees, M. M. Nojiri, D. P. Roy and Y. Yamada, Phys. Rev. **D56**, 276 (1997) [hep-ph/9701219].

[91] V. Barger and C. Kao, Phys. Rev. **D57**, 3131 (1998) [hep-ph/9704403].

[92] C. Boehm, A. Djouadi and M. Drees, Phys. Rev. **D62**, 035012 (2000) [hep-ph/9911496].

[93] A. Bottino, F. Donato, N. Fornengo and S. Scopel, Phys. Rev. **D62**, 056006 (2000) [hep-ph/0001309].

[94] J. L. Feng, K. T. Matchev and F. Wilczek, Phys. Lett. **B482**, 388 (2000) [hep-ph/0004043].

[95] J. L. Feng, K. T. Matchev and F. Wilczek, Phys. Rev. **D63**, 045024 (2001) [astro-ph/0008115].

[96] H. Baer, M. Brhlik, M. A. Díaz, J. Ferrandis, P. Mercadante, P. Quintana and X. Tata, Phys. Rev. **D63**, 015007 (2001) [hep-ph/0005027].

[97] J. Ellis, T. Falk, G. Ganis, K. A. Olive and M. Srednicki, hep-ph/0102098.

[98] T. Moroi and L. Randall, Nucl. Phys. **B570**, 455 (2000) [hep-ph/9906527].

[99] B. Murakami and J. D. Wells, hep-ph/0011082.

[100] A. Birkedal-Hansen and B. D. Nelson, hep-ph/0102075.

[101] H. E. Haber and R. Hempfling, Phys. Rev. Lett. **66**, 1815 (1991).

[102] M. S. Berger, Phys. Rev. **D41**, 225 (1990).

[103] Y. Okada, M. Yamaguchi and T. Yanagida, Prog. Theor. Phys. **85**, 1 (1991).

[104] J. Ellis, G. Ridolfi and F. Zwirner, Phys. Lett. **B257**, 83 (1991).

[105] R. Barbieri and M. Frigeni, Phys. Lett. **B258**, 395 (1991).

[106] H. E. Haber and R. Hempfling, Phys. Rev. **D48**, 4280 (1993) [hep-ph/9307201].

[107] P. Chankowski, S. Pokorski and J. Rosiek, Nucl. Phys. **B423**, 437 (1994) [hep-ph/9303309].

[108] A. Dabelstein, Z. Phys. **C67**, 495 (1995) [hep-ph/9409375].

[109] A. Dabelstein, Nucl. Phys. **B456**, 25 (1995) [hep-ph/9503443].

[110] D. M. Pierce, J. A. Bagger, K. Matchev and R. Zhang, Nucl. Phys. **B491**, 3 (1997) [hep-ph/9606211].

[111] S. Heinemeyer, W. Hollik and G. Weiglein, Phys. Rev. **D58**, 091701 (1998) [hep-ph/9803277].

[112] S. Heinemeyer, W. Hollik and G. Weiglein, Phys. Lett. **B440**, 296 (1998) [hep-ph/9807423].

[113] S. Heinemeyer, W. Hollik and G. Weiglein, Eur. Phys. J. **C9**, 343 (1999) [hep-ph/9812472].

[114] S. Heinemeyer, W. Hollik and G. Weiglein, Phys. Lett. **B455**, 179 (1999) [hep-ph/9903404].

[115] M. Carena, H. E. Haber, S. Heinemeyer, W. Hollik, C. E. Wagner and G. Weiglein, Nucl. Phys. **B580**, 29 (2000) [hep-ph/0001002].

[116] J. A. Casas, J. R. Espinosa, M. Quiros and A. Riotto, Nucl. Phys. **B436**, 3 (1995) [hep-ph/9407389].

[117] M. Carena, J. R. Espinosa, M. Quiros and C. E. Wagner, Phys. Lett. **B355**, 209 (1995) [hep-ph/9504316].

[118] M. Carena, M. Quiros and C. E. Wagner, Nucl. Phys. **B461**, 407 (1996) [hep-ph/9508343].

[119] H. E. Haber, R. Hempfling and A. H. Hoang, Z. Phys. **C75**, 539 (1997) [hep-ph/9609331].

[120] R. Hempfling and A. H. Hoang, Phys. Lett. **B331**, 99 (1994) [hep-ph/9401219].

[121] R. Zhang, Phys. Lett. **B447**, 89 (1999) [hep-ph/9808299].

[122] J. R. Espinosa and R. Zhang, Nucl. Phys. **B586**, 3 (2000) [hep-ph/0003246].

[123] M. Acciarri *et al.* [L3 Collaboration], Phys. Lett. **B495**, 18 (2000) [hep-ex/0011043].

[124] R. Barate *et al.* [ALEPH Collaboration], Phys. Lett. **B495**, 1 (2000) [hep-ex/0011045].

[125] G. Abbiendi *et al.* [OPAL Collaboration], Phys. Lett. **B499**, 38 (2001) [hep-ex/0101014].

[126] P. Abreu *et al.* [DELPHI Collaboration], Phys. Lett. **B499**, 23 (2001) [hep-ex/0102036].

[127] J. Ellis, G. Ganis, D. V. Nanopoulos and K. A. Olive, hep-ph/0009355.

[128] S. Su, Nucl. Phys. **B573**, 87 (2000) [hep-ph/9910481].

[129] G. L. Kane, S. F. King and L. Wang, hep-ph/0010312.

[130] A. Djouadi, P. Gambino, S. Heinemeyer, W. Hollik, C. Junger and G. Weiglein, Phys. Rev. Lett. **78**, 3626 (1997) [hep-ph/9612363].

[131] A. Djouadi, P. Gambino, S. Heinemeyer, W. Hollik, C. Junger and G. Weiglein, Phys. Rev. **D57**, 4179 (1998) [hep-ph/9710438].

[132] J. Erler and D. M. Pierce, Nucl. Phys. **B526**, 53 (1998) [hep-ph/9801238].

[133] G. Cho and K. Hagiwara, Nucl. Phys. **B574**, 623 (2000) [hep-ph/9912260].

[134] G. Cho, K. Hagiwara and M. Hayakawa, Phys. Lett. **B478**, 231 (2000) [hep-ph/0001229].

[135] J. Erler, S. Heinemeyer, W. Hollik, G. Weiglein and P. M. Zerwas, Phys. Lett. **B486**, 125 (2000) [hep-ph/0005024].

[136] H. N. Brown *et al.* [Muon g-2 Collaboration], Phys. Rev. Lett. **86**, 2227 (2001) [hep-ex/0102017].

[137] J. A. Grifols and A. Mendez, Phys. Rev. **D26**, 1809 (1982).

[138] J. Ellis, J. Hagelin and D. V. Nanopoulos, Phys. Lett. **B116**, 283 (1982).

[139] R. Barbieri and L. Maiani, Phys. Lett. **B117**, 203 (1982).

[140] D. A. Kosower, L. M. Krauss and N. Sakai, Phys. Lett. **B133**, 305 (1983).

[141] T. C. Yuan, R. Arnowitt, A. H. Chamseddine and P. Nath, Z. Phys. **C26**, 407 (1984).

[142] A. Czarnecki and W. J. Marciano, hep-ph/0102122.

[143] L. Everett, G. L. Kane, S. Rigolin and L. Wang, hep-ph/0102145.

[144] J. L. Feng and K. T. Matchev, Phys. Rev. Lett. **86**, 3480 (2001) [hep-ph/0102146].

[145] E. A. Baltz and P. Gondolo, hep-ph/0102147.

[146] U. Chattopadhyay and P. Nath, hep-ph/0102157.

[147] S. Komine, T. Moroi and M. Yamaguchi, hep-ph/0102204.

[148] H. Baer, C. Balazs, J. Ferrandis and X. Tata, hep-ph/0103280.

[149] J. Hisano and K. Tobe, hep-ph/0102315.

[150] T. Ibrahim, U. Chattopadhyay and P. Nath, hep-ph/0102324.

[151] J. Ellis, D. V. Nanopoulos and K. A. Olive, hep-ph/0102331.

[152] K. Choi, K. Hwang, S. K. Kang, K. Y. Lee and W. Y. Song, hep-ph/0103048.

[153] S. P. Martin and J. D. Wells, hep-ph/0103067.

[154] T. Tsukamoto, K. Fujii, H. Murayama, M. Yamaguchi, and Y. Okada, Phys. Rev. **D51**, 3153 (1995).

[155] J. L. Feng, M. E. Peskin, H. Murayama and X. Tata, Phys. Rev. **D52**, 1418 (1995) [hep-ph/9502260].

[156] D. G. Cassel, L. Trindle Gennari, R. H. Siemann, editors "DPF/DPB Summer Study on New Directions for High-Energy Physics (Snowmass 96), Snowmass, CO, 25 Jun - 12 Jul 1996. NEW DIRECTIONS FOR HIGH-ENERGY PHYSICS: Proceedings."

[157] E. Goodman, COLO-HEP-398, `http://hep-www.colorado.edu/SUSY`.

[158] H. Baer, F. E. Paige, S. D. Protopopescu and X. Tata, hep-ph/0001086.

[159] J. Dunn, "Study of the Detector Response to a Selectron Signal at the NLC," COLO-HEP-461, in preparation.

[160] E. Goodman, COLO-HEP-455, `http://hep-www.colorado.edu/SUSY`.

[161] B. Williams, COLO-HEP-402, `http://hep-www.colorado.edu/SUSY`.

[162] N. Danielson, COLO-HEP-404, `http://hep-www.colorado.edu/SUSY`.

[163] H. Baer, R. Munroe and X. Tata, Phys. Rev. **D54**, 6735 (1996) [hep-ph/9606325].

[164] "Supersymmetry, Chapter 3 of TESLA TDR", DESY-2001-011, ECFA-2001-209.

[165] J. Barron "Finding the Mass of the Chargino and the Sneutrino at the NLC," COLO-HEP-459, in preparation.

[166] C. Veeneman "Study of the Decay $\widetilde{\chi}_2^{\pm} \rightarrow \widetilde{\chi}_1^{\pm} Z^0$ with decays $\rightarrow q\overline{q}l^+l^-$ at the NLC,"COLO-HEP-463, in preparation.

[167] M. Dima, "Susy $\widetilde{e}_{R,L}^{\pm}/\widetilde{\mu}_{R,L}^{\pm}$ Studies, COLO-HEP-454," Talk presented at LCWS 2000, Fermilab, October, 2000; `http://hep-www.colorado.edu/SUSY`.

[168] N. Danielson and E. Goodman, COLO-HEP-422, `http://hep-www.colorado.edu/SUSY`.

[169] T. W. Markiewicz, T. Maruyama, "Interaction region issues at the NLC," Proceedings of the Worldwide Study on Physics and Experiments with Future Linear e^+e^- Linear Colliders, Sitges, Barcelona, Spain, April 1999.

[170] N. Danielson and B. Newman, COLO-HEP-428, `http://hep-www.colorado.edu/SUSY`.

[171] R. Kelly and C. Takeuchi, COLO-HEP-450, `http://hep-www.colorado.edu/SUSY`.

[172] J. Barron, COLO-HEP-449, `http://hep-www.colorado.edu/SUSY`.

[173] D. Staszak,"Studies of a Smuon Signal in a NLC Detector," COLO-HEP-460, in preparation.

[174] H. Martyn and G. A. Blair, hep-ph/9910416.

[175] J. L. Feng and D. E. Finnell, Phys. Rev. **D49**, 2369 (1994) [hep-ph/9310211].

[176] David Wagner, COLO-HEP-400, `http://hep-www.colorado.edu/SUSY`.

[177] David Wagner, COLO-HEP-401, `http://hep-www.colorado.edu/SUSY`.

[178] H. Baer, J. K. Mizukoshi, and X. Tata, private communication.

[179] J. F. Gunion and S. Mrenna, hep-ph/0103167.

[180] H. Baer, C. Balazs, S. Hesselbach, J. K. Mizukoshi and X. Tata, hep-ph/0012205.

[181] S. Y. Choi, A. Djouadi, M. Guchait, J. Kalinowski, H. S. Song and P. M. Zerwas, Eur. Phys. J. **C14**, 535 (2000) [hep-ph/0002033].

[182] G. Moortgat-Pick, A. Bartl, H. Fraas and W. Majerotto, Eur. Phys. J. **C18**, 379 (2000) [hep-ph/0007222].

[183] M. M. Nojiri, K. Fujii and T. Tsukamoto, Phys. Rev. **D54**, 6756 (1996) [hep-ph/9606370].

[184] A. Bartl, H. Eberl, S. Kraml, W. Majerotto, W. Porod and A. Sopczak, Z. Phys. **C76**, 549 (1997) [hep-ph/9701336].

[185] H. Baer, C. Balazs, J. K. Mizukoshi and X. Tata, Phys. Rev. **D63**, 055011 (2001) [hep-ph/0010068].

[186] M. M. Nojiri, K. Fujii and T. Tsukamoto, *Prepared for 6th Workshop on the Japan Linear Collider (JLC), Tokyo, Japan, 4-5 Dec 1996*, Phys. Rev. **D54**, 6756 (1886).

[187] K. Hikasa and T. Nagano, Phys. Lett. **B435**, 67 (1998) [hep-ph/9805246].

[188] J. L. Feng and T. Moroi, Phys. Rev. **D56**, 5962 (1997) [hep-ph/9612333].

[189] V. Barger, T. Han and J. Jiang, hep-ph/0006223.

[190] K. Hikasa and Y. Nakamura, Z. Phys. **C70**, 139 (1996) [hep-ph/9501382]; erratum, Z. Phys. **C71**, 356 (1996).

[191] P. H. Chankowski, Phys. Rev. **D41**, 2877 (1990).

[192] M. E. Peskin and T. Takeuchi, Phys. Rev. Lett. **65**, 964 (1990).

[193] H. Cheng, J. L. Feng and N. Polonsky, Phys. Rev. **D56**, 6875 (1997) [hep-ph/9706438].

[194] H. Cheng, J. L. Feng and N. Polonsky, Phys. Rev. **D57**, 152 (1998) [hep-ph/9706476].

[195] M. M. Nojiri, D. M. Pierce and Y. Yamada, Phys. Rev. **D57**, 1539 (1998) [hep-ph/9707244].

[196] E. Katz, L. Randall and S. Su, Nucl. Phys. **B536**, 3 (1998) [hep-ph/9801416].

[197] S. Kiyoura, M. M. Nojiri, D. M. Pierce and Y. Yamada, Phys. Rev. **D58**, 075002 (1998) [hep-ph/9803210].

[198] M. A. Díaz, S. F. King and D. A. Ross, Nucl. Phys. **B529**, 23 (1998) [hep-ph/9711307].

[199] M. A. Díaz, S. F. King and D. A. Ross, hep-ph/0008117.

[200] T. Blank and W. Hollik, hep-ph/0011092.

[201] S. Y. Choi, M. Guchait, J. Kalinowski and P. M. Zerwas, Phys. Lett. **B479**, 235 (2000) [hep-ph/0001175].

[202] U. Mahanta, Phys. Rev. **D59**, 015017 (1999) [hep-ph/9810344].

[203] H. Dreiner, hep-ph/9707435.

[204] G. Bhattacharyya, hep-ph/9709395.

[205] G. Bhattacharyya, Nucl. Phys. Proc. Suppl. **52A**, 83 (1997) [hep-ph/9608415].

[206] M. Bisset, O. C. Kong, C. Macesanu and L. H. Orr, Phys. Lett. **B430**, 274 (1998) [hep-ph/9804282].

[207] L. J. Hall and M. Suzuki, Nucl. Phys. **B231**, 419 (1984).

[208] D. K. Ghosh, R. M. Godbole and S. Raychaudhuri, hep-ph/9904233.

[209] D. K. Ghosh, R. M. Godbole and S. Raychaudhuri, Z. Phys. **C75**, 357 (1997) [hep-ph/9605460].

[210] R. Barate *et al.* [ALEPH Collaboration], Phys. Lett. **B420**, 196 (1998).

[211] F. de Campos, M. A. Garcia-Jareno, A. S. Joshipura, J. Rosiek and J. W. Valle, Nucl. Phys. **B451**, 3 (1995) [hep-ph/9502237].

[212] T. Banks, Y. Grossman, E. Nardi and Y. Nir, Phys. Rev. **D52**, 5319 (1995) [hep-ph/9505248].

[213] A. Y. Smirnov and F. Vissani, Nucl. Phys. **B460**, 37 (1996) [hep-ph/9506416].

[214] H. Nilles and N. Polonsky, Nucl. Phys. **B484**, 33 (1997) [hep-ph/9606388].

[215] M. A. Diaz, J. C. Romao and J. W. Valle, Nucl. Phys. **B524**, 23 (1998) [hep-ph/9706315].

[216] R. Hempfling, Nucl. Phys. **B478**, 3 (1996) [hep-ph/9511288].

[217] E. J. Chun and S. K. Kang, Phys. Rev. **D61**, 075012 (2000) [hep-ph/9909429]; E. J. Chun, Phys. Lett. **B505**, 155 (2001) [hep-ph/0101170].

[218] M. Hirsch, M. A. Diaz, W. Porod, J. C. Romao and J. W. Valle, Phys. Rev. **D62**, 113008 (2000) [hep-ph/0004115].

[219] J. C. Romao, M. A. Diaz, M. Hirsch, W. Porod and J. W. Valle, Phys. Rev. **D61**, 071703 (2000) [hep-ph/9907499].

[220] W. Porod, M. Hirsch, J. Romao and J. W. Valle, hep-ph/0011248.

[221] N. Arkani-Hamed, H. Cheng, J. L. Feng and L. J. Hall, Phys. Rev. Lett. **77**, 1937 (1996) [hep-ph/9603431].

[222] N. Arkani-Hamed, J. L. Feng, L. J. Hall and H. Cheng, Nucl. Phys. **B505**, 3 (1997) [hep-ph/9704205].

[223] J. Hisano, M. M. Nojiri, Y. Shimizu and M. Tanaka, Phys. Rev. **D60**, 055008 (1999) [hep-ph/9808410].

[224] J. J. Cao, T. Han, X. Zhang and G. R. Lu, Phys. Rev. **D59**, 095001 (1999) [hep-ph/9808466].

[225] D. Nomura, hep-ph/0004256.

[226] M. Guchait, J. Kalinowski and P. Roy, hep-ph/0103161.

[227] M. Dugan, B. Grinstein and L. Hall, Nucl. Phys. **B255**, 413 (1985).

[228] T. Ibrahim and P. Nath, Phys. Rev. **D58**, 111301 (1998) [hep-ph/9807501].

[229] M. Brhlik, G. J. Good and G. L. Kane, Phys. Rev. **D59**, 115004 (1999) [hep-ph/9810457].

[230] D. Atwood, S. Bar-Shalom, G. Eilam and A. Soni, hep-ph/0006032.

[231] B. Grzadkowski, Phys. Lett. **B305**, 384 (1993) [hep-ph/9303204].

[232] A. Bartl, E. Christova, T. Gajdosik and W. Majerotto, Nucl. Phys. **B507**, 35 (1997) [hep-ph/9705245].

[233] S. Y. Choi, A. Djouadi, H. S. Song and P. M. Zerwas, Eur. Phys. J. **C8**, 669 (1999) [hep-ph/9812236].

[234] J. L. Kneur and G. Moultaka, Phys. Rev. **D61**, 095003 (2000) [hep-ph/9907360].

[235] V. Barger, T. Han, T. Li and T. Plehn, Phys. Lett. **B475**, 342 (2000) [hep-ph/9907425].

[236] V. Barger, T. Falk, T. Han, J. Jiang, T. Li and T. Plehn, hep-ph/0101106.

[237] W. Y. Keung and L. Littenberg, Phys. Rev. **D28**, 1067 (1983).

[238] J. L. Feng, Int. J. Mod. Phys. **A13**, 2319 (1998) [hep-ph/9803319].

[239] K. A. Thompson, Int. J. Mod. Phys. **A15**, 2485 (2000).

[240] J. L. Feng and M. E. Peskin, hep-ph/0105100.

[241] C. Bloechinger and W. Porod, in preparation.

[242] V. Barger, T. Han and J. Kelly, Phys. Lett. **B419**, 233 (1998) [hep-ph/9709366].

[243] D. Choudhury and F. Cuypers, Nucl. Phys. **B451**, 16 (1995) [hep-ph/9412245].

[244] K. Kiers, J. N. Ng and G. Wu, Phys. Lett. **B381**, 177 (1996) [hep-ph/9604338].

[245] S. Berge, M. Klasen and Y. Umeda, Phys. Rev. **D63**, 035003 (2001) [hep-ph/0008081].

[246] T. Mayer and H. Fraas, hep-ph/0009048.

[247] H. Baer, V. Barger, D. Karatas and X. Tata, Phys. Rev. **D36**, 96 (1987).

[248] S. Abdullin *et al.* [CMS Collaboration], hep-ph/9806366.

[249] H. Baer, P. G. Mercadante, F. Paige, X. Tata and Y. Wang, Phys. Lett. **B435**, 109 (1998) [hep-ph/9806290].

[250] H. Baer, P. G. Mercadante, X. Tata and Y. Wang, Phys. Rev. **D62**, 095007 (2000) [hep-ph/0004001].

[251] H. Baer, J. K. Mizukoshi and X. Tata, Phys. Lett. **B488**, 367 (2000) [hep-ph/0007073].

[252] ATLAS Collaboration, *ATLAS Detector and Physics Performance Technical Design Report*, CERN/LHCC/99-14, `http://atlasinfo.cern.ch/Atlas/-GROUPS/PHYSICS/TDR/access.html`.

[253] H. Baer, C. Chen, F. Paige and X. Tata, Phys. Rev. **D52**, 2746 (1995) [hep-ph/9503271].

[254] H. Baer, C. Chen, F. Paige and X. Tata, Phys. Rev. **D53**, 6241 (1996) [hep-ph/9512383].

[255] H. Baer, C. Chen and X. Tata, Phys. Rev. **D55**, 1466 (1997) [hep-ph/9608221].

[256] I. Hinchliffe, F. E. Paige, M. D. Shapiro, J. Soderqvist and W. Yao, Phys. Rev. **D55**, 5520 (1997) [hep-ph/9610544].

[257] H. Baer, C. Chen, F. Paige and X. Tata, Phys. Rev. **D50**, 4508 (1994) [hep-ph/9404212].

[258] H. Bachacou, I. Hinchliffe and F. E. Paige, Phys. Rev. **D62**, 015009 (2000) [hep-ph/9907518].

[259] B. C. Allanach, C. G. Lester, M. A. Parker and B. R. Webber, JHEP **0009**, 004 (2000) [hep-ph/0007009].

[260] H. Baer, C. Chen, M. Drees, F. Paige and X. Tata, Phys. Rev. **D59**, 055014 (1999) [hep-ph/9809223].

[261] D. R. Tovey, hep-ph/0006276.

[262] H. Baer, C. Chen, F. Paige and X. Tata, Phys. Rev. **D49**, 3283 (1994) [hep-ph/9311248].